TETRAPHOSPHINE LINKER SCAFFOLDS WITH A TETRAPHENYLTIN CORE FOR SUPERIOR IMMOBILIZED CATALYSTS: A SOLID-STATE NMR STUDY

A Thesis

by

MELANIE INGRID PERERA

Submitted to the Office of Graduate Studies of
Texas A&M University
in partial fulfillment of the requirements for the degree of

MASTER OF SCIENCE

August 2011

Major Subject: Chemistry

Tetraphosphine Linker Scaffolds with a Tetraphenyltin Core for Superior Immobilized Catalysts: A Solid-State NMR Study

TETRAPHOSPHINE LINKER SCAFFOLDS WITH A TETRAPHENYLTIN CORE FOR SUPERIOR IMMOBILIZED CATALYSTS: A SOLID-STATE NMR STUDY

A Thesis

by

MELANIE INGRID PERERA

Submitted to the Office of Graduate Studies of
Texas A&M University
in partial fulfillment of the requirements for the degree of

MASTER OF SCIENCE

Approved by:

Co-Chairs of Committee,	Janet Bluemel
	Francois P. Gabbai
Committee Members,	Simon W. North
	Tatyana I. Igumenova
Head of Department,	David H. Russell

August 2011

Major Subject: Chemistry

ABSTRACT

Tetraphosphine Linker Scaffolds with a Tetraphenyltin Core for Superior Immobilized Catalysts: A Solid-State NMR Study. (August 2011)

Melanie Ingrid Perera, B.S., Wheeling Jesuit

Co-Chairs of Advisory Committee: Dr. Janet Bluemel
Dr. Francois P. Gabbai

The focus of this work is to synthesize and immobilize novel rigid tetraphosphine linkers via the formation of phosphonium groups and by direct adsorption of tetraphosphine salts on oxide surfaces. These methods offer the possibility to study the mechanism of the phosphonium formation in more detail by utilizing solid-state NMR spectroscopy. It has also been a point of interest to study the linkers and catalysts under realistic conditions, in the presence of solvents. Therefore, HRMAS (high-resolution magic angle spinning) NMR spectra of several phosphonium salts, adsorbed on SiO_2, have been studied. This technique allows one to probe the leaching and mobility of the linkers on the surface. The mobilities of the linkers and the catalysts are crucial factors for the performance and design of the immobilized catalysts. Finally, since the exact mode of binding to the surface is unknown and is being discussed in the literature, for example, as hydrogen bonding between the F atoms in BF_4^- and surface silanol protons, the influence of the counteranion on the binding of phosphonium salts on silica surfaces is of utmost interest. For surface mobility studies a monolayer of phosphonium salts on the silica surface, both without solvent and in the presence of solvent, has been studied

via ^{31}P and ^{2}H CP/MAS and HRMAS. Our findings show that the integrity of the tetraphosphine scaffold linkers is based upon how it is immobilized. The best system is formed when the phosphine is immobilized on the SiO_2 support by adding $Cl(CH_2)_3Si(OEt)_3$ to the reaction mixture. In this way, phosphonium salts are obtained, which are bound to the surface irreversibly by electrostatic interactions, as proven by solid-state NMR. In addition, leaching and mobility studies prove that the solvents play a crucial role, and the more polar solvents, such as DMSO, lead to the most extensive leaching due to the solvents' strong adsorption on the SiO_2 surface. Leaching studies also show that the counteranion has an influence on the binding of the phosphoniumn salts on the SiO_2 surface. The leaching proceeds in the following manner: $BF_4^- > I^- > Br^- > Cl^-$. This is an indication that there is an additional interaction between the anion and, most probably, the surface silanol protons.

DEDICATION

I dedicate this thesis to my family:

Especially my parents for being behind me 100% in all my endeavors. The love that has been shown to me can compare to no other;

To my brother, sister, and cousins for always keeping me smiling even at the roughest times;

To Stephen, for always supporting and encouraging me;

To my uncle Paul, who always reminded me of God's presence and the power of prayers.

I love you all.

Last, but not least, I dedicate this to my friends for always offering a shoulder to lean on.

ACKNOWLEDGEMENTS

I thank the National Science Foundation (NSF, CHE-0911207) for financing my salary, including tuition and fees, and the equipment, NMR time, and chemicals I used for working on my project.

I would like to thank my committee chair, Dr. Bluemel, and my committee members, Dr. Gabbai, Dr. North, and Dr. Igumenova, for their guidance and support throughout the course of this research.

Thanks also go to my friends and colleagues and the department faculty and staff for making my time at Texas A&M University a great experience. Finally, thanks to my mother and father for their encouragement, patience and love.

NOMENCLATURE

ADP	ammonium dihydrogen phosphate
AMP	adenosine monophosphate
B	magnetic field in Tesla
CP	cross polarization
CSA	chemical shift anisotropy
δ	chemical shift
DCM	dichloromethane
DED	dutch elm disease
dist.	distilled
DMSO	dimethylsulfoxide
E	quadrupolar interactions
EnCat	encapsulation
EtOH	ethanol
eq.	equivalent
exc.	excess
Et	ethyl
Et_2O	diethylether
FRPSG	fluorous reversed phase silica gel
h	hour
HP	high-power

HR	high resolution
HV	high vacuum
Hz	Hertz
kHz	kilohertz
MAS	magic angle spinning
Me	methyl
MeOH	methanol
min.	minute
mp.	melting point
NMR	nuclear magnetic resonance
ns	number of scans
Θ	surface coverage
p15	contact time for CP measurements
Ph	phenyl
PMMA	polymethylmethacrylate-d_8
ppm	parts per million
Q	quadrupolar moment
Q_{cc}	quadrupolar coupling constant
RT	room temperature
SAPC	supported aqueous phase catalysis
SLPC	supported liquid phase catalysis
SPOO	solid-phase organic synthesis

THF	tetrahydrofuran
TPPTS	triphenylphosphinetrisulphonate
T_1	longitudinal relaxation
ν_{rot}	rotational frequency

TABLE OF CONTENTS

Page

LIST OF FIGURES

FIGURE Page

FIGURE Page

LIST OF TABLES

LIST OF SCHEMES

1. INTRODUCTION

Immobilized species are important in such diverse areas as combinatorial chemistry,[1] solid-phase synthesis,[2] chromatography,[3] and catalysis.[4,5]Immobilized catalysts[4-6] are of immense academic and industrial interest, because they can combine the advantages of homogeneous catalysts, which include high activity and selectivity, with those of heterogeneous catalysts with their easy recyclability. Immobilized catalysts are highly active and selective, while they can be easily separated from the reaction mixtures and reused, for example, in subsequent batchwise catalysis cycles.[5,6] Research efforts in this field have been lacking due to insufficient analytical techniques for the study and characterization of surface-bound species. The most widely used technique has been infrared spectroscopy (IR), which provides structural information in the case of immobilized species with characteristic infrared adsorptions.[7] Solid-state NMR is another technique for analyzing these amorphous materials, but the first publications on studying complexes immobilized via linkers with solid-state NMR by Fyfe[8] remained the only articles of this kind for many years. However, in the meantime, solid-state NMR has evolved as a routine technique,[8,9] for example, with the development of high-power decoupling (HPDEC),[8] cross-polarization (CP),[10] and magic angle spinning (MAS)[10,11] techniques, which has allowed for the further development of this field. In our group, the most favorable support materials are silica and neutral alumina,[3,12]

This thesis follows the style of the *Journal of the American Chemical Society.*

and bifunctional phosphines, such as $Ph_2P(CH_2)_3Si(OEt)_3$, or the chelating phosphine $Ph_2P(CH_2)_3PPh(CH_2)_3Si(OEt)_3$, are popular linkers.[12,13] The latter, for example, has led to very successful immobilized nickel[14] and rhodium[15] catalysts for the cyclotrimerization of acetylenes and olefin hydrogenation, respectively.

The most promising system is a new generation of rigid linkers.[16] Catalysts immobilized by these linkers have prolonged lifetimes as compared to molecular catalysts tethered with flexible alkyl chain linkers. They can be recycled many more times.[6] Studies on the mobility of the linker systems under *in situ* conditions in the presence of a solvent will additionally enhance the basic understanding of surface phenomena, which have an impact on catalysis at the solid/liquid interface.

Oxides as supports provide many advantages as compared to polymers. For example, their pore size in different solvents is constant,[12] a parameter that is difficult to control with swellable polymers. Therefore, for the presented investigation porous oxide supports have been used, so that the mobility results are not blurred by any pore size variation depending on the solvents applied. Oxides are furthermore chemically and thermally stable in organic solvents, and their thermal conductivity prevents local overheating effects. From a practical point of view, it is favorable that oxides, especially with large particle diameters, settle down quickly after the catalytic reaction, and the supernatant can easily be decanted without filtration or centrifugation. Because of these obvious advantages of oxide supports, the scope of this project will be mostly limited to species immobilized on oxide supports, such as silica. For the mobility studies all systems of the tetraphosphine and phosphonium type (Figure1-1) with Sn as the center

atom, will be immobilized on mesoporous silica (Merck silica, average pore diameter 40 Å, specific surface area 750 m^2/g), which has been used previously.

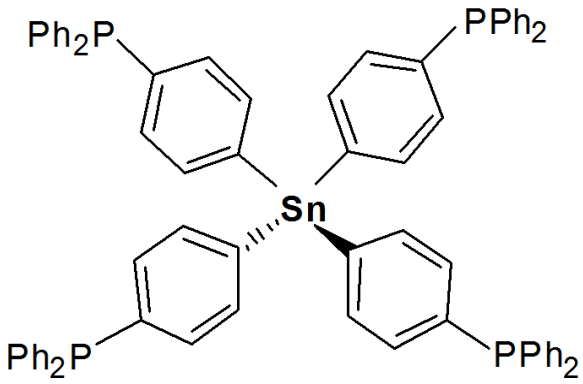

Figure 1-1. Tetraphosphine with a tetraphenyltin scaffold.

Since both linkers and catalysts immobilized on oxide supports are amorphous materials, solid-state NMR has turned out to be the most versatile and powerful analytical tool in our group although other analytical methods for solids are readily available as well.[17,18]

2. BACKGROUND

2.1 Solid-State NMR

A basic analytical method for the characterization of insoluble and amorphous solid materials is solid-state NMR. It offers an attractive alternative for the structural characterization of amorphous and crystalline solids to other methods, like X-ray diffraction and mass spectrometry. It is also a suitable method for the characterization of immobilized compounds on inorganic supports. Because of the molecules' isotropic reorientation in solution, in an NMR experiment of a dissolved substance the resonance frequency is the average value of all possible orientations with respect to the external magnetic field. In a solid, however, a molecule has a specific position in the external magnetic field and different anisotropic interactions are not averaged out and can be observed.[19] All interactions can be described with the associated Hamiltonian operators. In an NMR experiment, the total Hamiltonian operator $\hat{H}$ is the sum of all Hamiltonian operators of the separate interactions, as seen in the following:

$$\hat{H} = \hat{H}_Z + \hat{H}_Q + \hat{H}_D + \hat{H}_g + \hat{H}_{CS} + \hat{H}_J$$

With $\hat{H}_Z$ = Zeeman Interaction

$\hat{H}_Q$ = Quadrupolar Interactions

$\hat{H}_D$ = Dipolar Interactions

$\hat{H}_g$ = Interactions with unpaired electron spins

$\hat{H}_{CS}$ = Chemical Shift Anisotropy

$\hat{H}_J$ = Scalar Coupling

The Zeeman interaction describes the splitting of previously degenerate energy levels in an external magnetic field. The basis of every NMR experiment is to excite nuclear spins of lower energy levels to occupy higher energy levels via electromagnetic radiation in the radio frequency range. The observed relaxation is the FID (Free Induction Decay), which results in the NMR spectrum after FT (Fourier Transformation) of the data. Only the Zeeman interaction is isotropic, all the others are not spherically symmetric. Table 2-1 gives an overview of the range and the dependence of the respective interactions from the external magnetic field (B_0).

Table 2-1. Overview of the maximal/average range and the dependence of the anisotropic interactions in the solid state from the external magnetic field (B_0).

Interaction	Dependence regarding B_0	Typical Range
$\hat{H}_Z$	~ B_0	50 MHz
$\hat{H}_Q$	1st order H_Q independent of B_0, 2nd order H_Q ~ 1/ B_0	5 MHz
$\hat{H}_D$	Independent of B_0	100 kHz
$\hat{H}_g$	Dependent on B_0 (complex)	100 kHz
$\hat{H}_{CS}$	~ B_0	20 kHz
$\hat{H}_J$	Independent of B_0	100 Hz

Chemical Shift Anisotropy

The Chemical Shift Anisotropy (CSA) is due to an electron surroundings of a nucleus, which is not spherically symmetric.[20] The nucleus is thus shielded in different ways, depending on the relative orientation of the external magnetic field with respect to the spatial electron distribution. For every orientation of the molecule, there is a separate shielding constant σ and an effective magnetic field $B_{eff} = (1- \sigma) B_0$ (Figure 2-1).

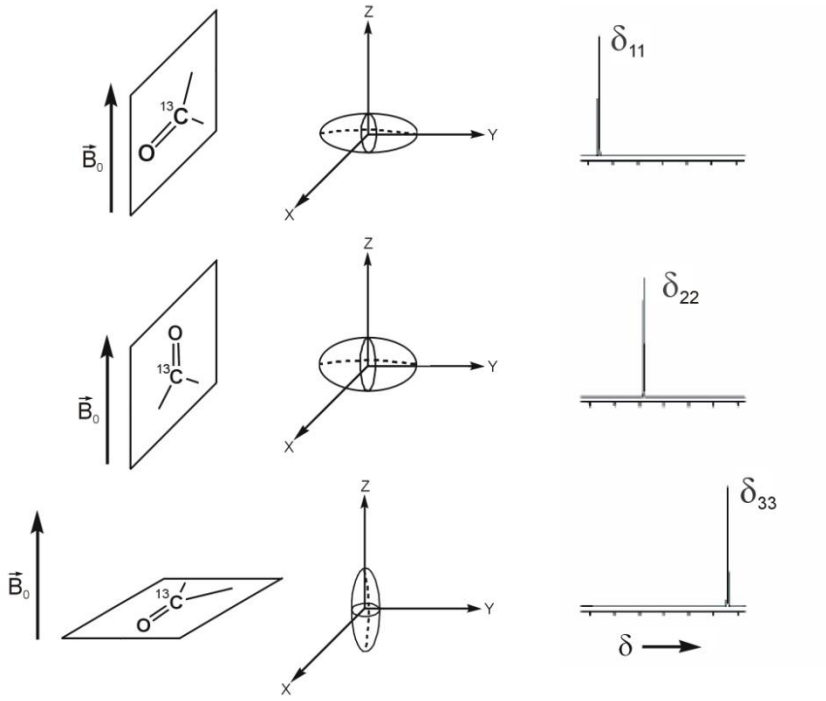

Figure 2-1. Schematic illustration of the primary values of the CSA in ^{13}C NMR using the example of a carbonyl group.[21]

Hence a wideline (or powder) spectrum of a solid is obtained. The turning points of the outer edge of the wideline spectrum are labeled as δ_{11} and δ_{33} (in the literature also

σ_{11} and σ_{33}).[20] The maximum of the intensity of the signal is assigned to δ_{22} (σ_{22}). The isotropic chemical shift δ_{iso}, which would also be found if the compound were dissolved and isotropically reorienting in solution, can be calculated as follows:

$$\delta_{iso} = 1/3\ (\delta_{11} + \delta_{22} + \delta_{33})$$

The isotropic chemical shift represents the center of gravity of the wideline signal (Figure 2-2). The appearance of the wideline spectrum is mostly defined by the relative position of δ_{22} between δ_{11} and δ_{33}. δ_{22} can either overlap with δ_{11} or δ_{33}, be in the center of the signal, or it can assume a random position between these two extremes.

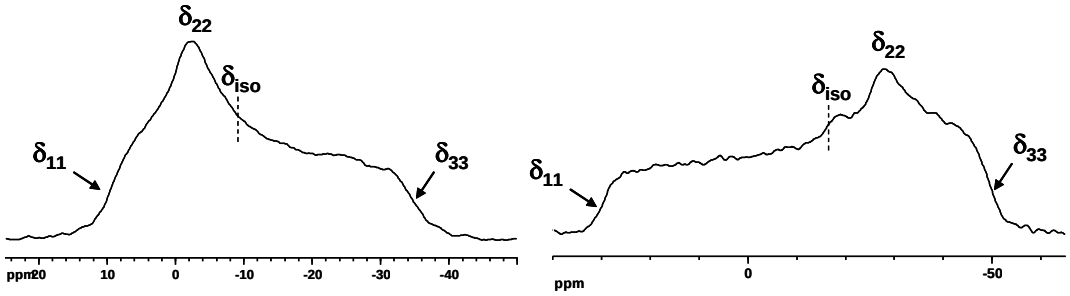

Figure 2-2. Two representative wideline spectra; ^{31}P NMR of compounds 4-(p-bromophenyl)phenyldiphenylphosphine (left) and 4-(p-bromophenyl)phenyl diethylphosphine (right).[22]

The two main disadvantages of wideline spectra are the large signal widths, and the resultant low signal intensities. The most effective method to reduce the lines of a solid-state NMR spectrum is MAS. The sample is rotated with high frequencies of

routinely up to 35 kHz at the so-called "Magic Angle" of $\theta = 54.7°$. In Figure 2-3 the principle of MAS is depicted schematically.

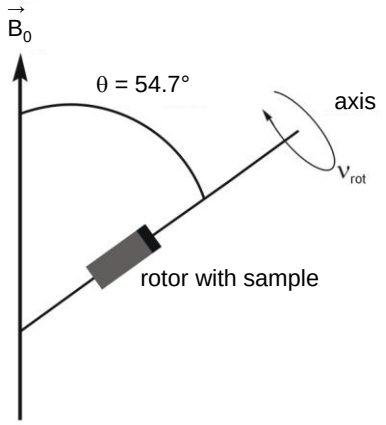

Figure 2-3. Schematic representation of MAS.

A detailed view on $\hat{H}_{CS}$ makes MAS understandable:

$$\hat{H}_{CS} = \gamma \cdot \hbar \cdot \vec{I}_z \cdot \hat{\sigma} \cdot \vec{B}_o$$

$$\hat{H}_{CS} = \gamma \cdot \hbar \cdot \vec{I}_z \cdot \delta_{iso} \cdot \vec{B}_o + (\gamma \cdot \hbar \cdot \vec{I}_z \cdot \vec{B}_o / 2) \cdot [(3 \cdot \cos^2\theta - 1) \cdot (\delta_{22} - \delta_{iso})] \cdot [\sin^2\theta \cdot \cos^2\psi \cdot (\delta_{22} - \delta_{11})]$$

with

	γ	=	Gyromagnetic ratio
	$\hbar$	=	(Planck constant)/$2\pi \approx 1.055 \cdot 10^{-34}$ Js
	$\hat{I}_z$	=	Nuclear spin component in magnetic field direction
	σ	=	Displacement tensor
	B_o	=	External magnetic field
	δ_{iso}	=	Isotropic chemical shift
	θ	=	Angle between rotational axis and B_o
	ψ	=	Rotational phase angle of the rotor

If the factor $(3\cos^2\theta - 1)$ becomes zero, then the above mathematical description of $\hat{H}_{CS}$ is highly simplified. In a spectrum this becomes noticeable, because instead of a wideline spectrum, isotropic chemical shifts and rotational sidebands are obtained. The distance between δ_{iso} and the rotational sidebands, as well as the distance of the rotational sidebands from each other, is equal to the rotational frequency of the rotor (Figure 2-4). The faster a sample is rotated, the larger the distance between the lines, and the larger the intensity of the isotropic line.

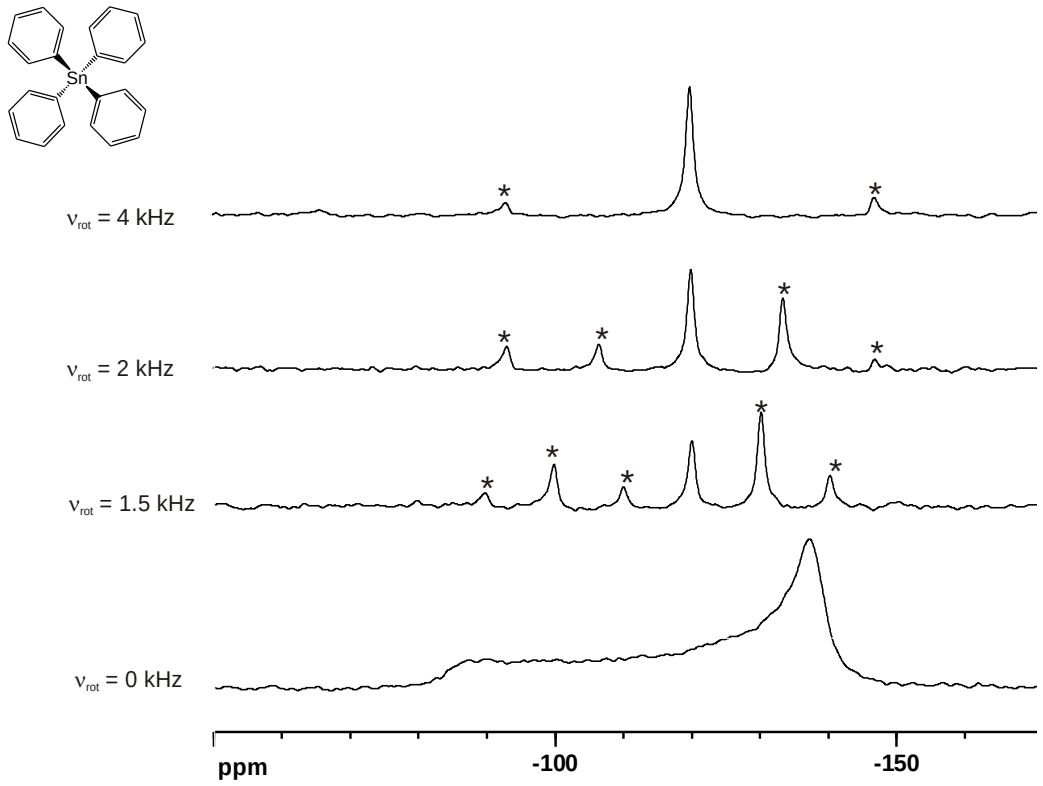

Figure 2-4. ^{119}Sn MAS NMR spectrum of tetraphenyltin at the indicated rotational speeds.[22] Asterisks denote rotational sidebands, the isotropic chemical shift is -120.0 ppm.

Dipolar Interactions

Other factors, which lead to broader signals in solid-state NMR spectra are dipolar interactions. These interactions occur through space and can be either homonuclear (interactions between nuclei of the same isotope) or heteronuclear (interactions between nuclei of different elements or isotopes). Dipolar interactions between two NMR-active nuclei can be described as the disturbance of the magnetic field of one nucleus by the magnetic dipolar field of another nucleus.[19] Quantitatively, the dipolar interactions can be described by the Hamiltonian operator $\hat{H}_D$.

$$\hat{H}_D = [\ (\gamma_A\ \gamma_E)/r^3]\cdot\hbar^2\cdot\vec{A}\cdot\hat{D}\cdot\vec{E}$$

$$\hat{H}_D = 0.5\cdot[\ \gamma_A\ \gamma_E)/r^3]\cdot\hbar^2\cdot(3\cdot\cos^2\theta - 1)\cdot(3\cdot A_Z\cdot E_Z - \vec{A}\cdot\vec{E})$$

With γ_A, γ_B = Gyromagnetic ratios of nuclei A and E

r = Distance between nuclei A and E

$\hbar$ = (Planck constant)/$2\pi \approx 1.05510^{-34}$ Js

$\vec{A}\cdot\vec{E}$ = Nuclear spin unit of nuclei A and E in direction of B_0

$\hat{D}$ = Tensor of dipolar coupling

Some major characteristics of dipolar interactions become obvious by the mathematical description of $\hat{H}_D$. For example, the extent of the dipolar interactions is dependent on the gyromagnetic ratio of the two nuclei and is proportional to $1/r^3$ (the dipolar interactions decrease with increasing distance of the interacting nuclei). Dipolar interactions are also independent of the external magnetic field B_0.

Cross Polarization

Besides the large spectral linedwidth and the small signal intensity, the long T_1 relaxation times and the resulting long measurement times are major drawbacks in solid-state NMR spectroscopy. Waugh, Pines, and Gibby found a solution for this problem in a transfer of magnetization from abundant nuclei like ^{1}H and ^{19}F to the observed nucleus.[23] This phenomenon is used in the "Cross Polarization" (CP) pulse sequence. In CP, the nuclear spin of the abundant nucleus is subjected to a 90° pulse around the x axis. Subsequently, the magnetizations of the abundant nuclei and the observed nucleus are retained in the x,y plane by a spin-lock field. During the contact time, which is in the range of 0.5 to 12 ms, magnetization is transferred from the abundant nuclei to the dilute nucleus. As a prerequisite for the magnetization to be transferred effectively, the Hartmann-Hahn condition has to be fulfilled:

$$\gamma(^{1}H)\, B_1(^{1}H) = \gamma(X)\, B_1(X)$$

Subsequently, the abundant nuclei are decoupled, while the FID of the less abundant nucleus is recorded. The strengths of the spinlock field and the field for ^{1}H decoupling have to be different in order to avoid interferences. After a short pulse delay time, which is now determined by the relaxation time of the abundant nuclei, the cycle begins again. The pulse sequence of the most basic CP experiment is presented in Figure 2-5.

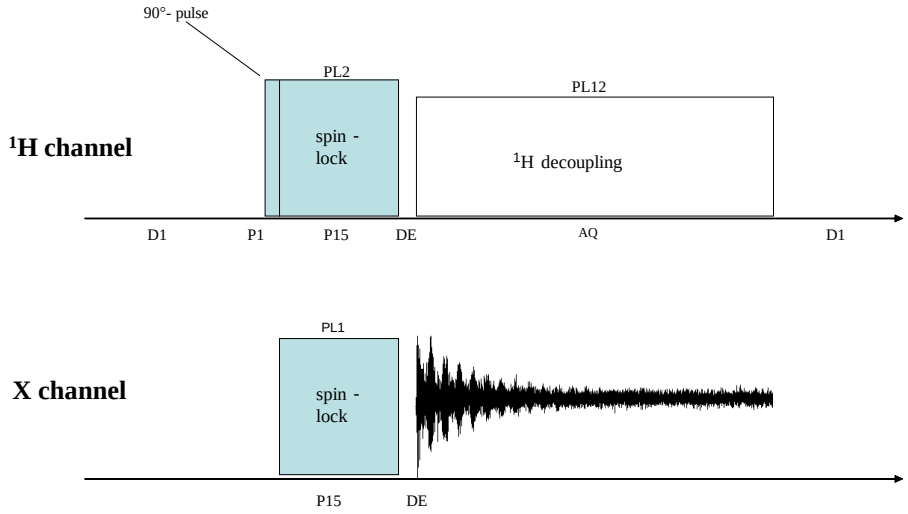

Figure 2-5. Schematic representation of pulse sequence for cross polarization.[22]

2.2 Deuterium NMR

About 70 % of all nuclei possess a nuclear spin I > ½, and therefore they are quadrupolar nuclei. The electric quadrupolar moment Q stems from an unsymmetrical distribution of charge within the nucleus. Thus the nuclei are not spherically symmetric. There are two possibilities for unsymmetric nuclei, which are represented by prolate and oblate nuclei. The prolate nucleus is longer in the direction of its nuclear spin angular momentum, giving it a cigar-type shape in which case Q > 0. The oblate nucleus is flattened like the earth and Q < 0. If one brings a quadrupolar nucleus into an inhomogeneous electric field, there will be an interaction with the electric field gradient and the energy contents of the quadrupolar nucleus is split into distinct levels (Figure 2-6).[19]

I = 1 (^{2}H, ^{6}Li, ^{14}N)

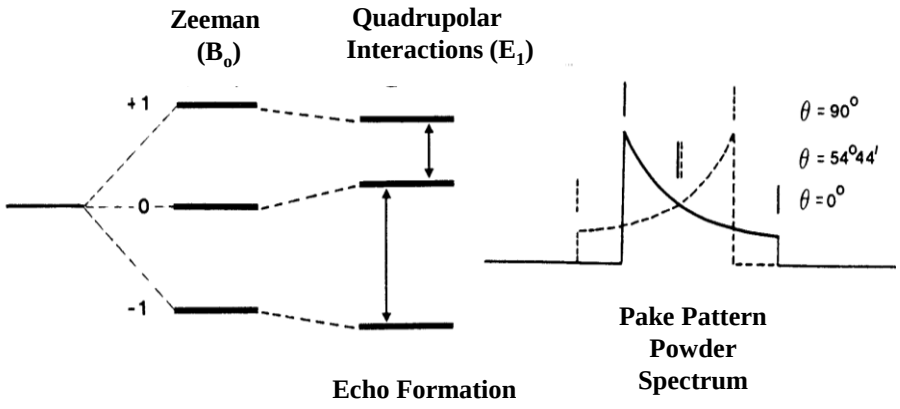

Figure 2-6. Scheme of first-order quadrupolar interactions (left) and resulting pake pattern (right).

Quadrupolar effects stem from the interactions of the electric field gradient with the quadrupolar nucleus. While these interactions are cancelled out by the rapid tumbling of the molecules in solution, in the solid state they still remain. There are two types of interactions: a) First Order Quadrupolar Interactions ($E^{(1)}$, E^{1}) ; in this case the quadrupolar coupling constant (Q_{cc}) is relatively small, as compared to the Zeeman interaction. In the presence of solely first order quadrupolar interactions, the signal shapes are simple, predictable, and easy to interpret and simulate. b) Second Order Quadrupolar Interactions ($E^{(2)}$, E^{2}); in this case the Q_{cc} is relatively large as compared to the Zeeman interaction. With second or higher order quadrupolar interactions the signals are unsymmetric, irregular, and very complex. They can hardly be predicted and each system needs special attention. Quadrupolar interactions are dependent on the nuclear

spin, I, and the Q_{cc}. For ^2H the signals span from about 170 kHz to 200 kHz. In the solid state, because of the presence of first order quadrupolar interactions, the splitting of the energy levels is unsymmetric and two resonances are expected.[24]

$\Delta E_Q = h \cdot 3/8\ (e^2qQ/h)(3\cos^2\theta - 1)$.

Hereby, the factor (e^2qQ/h) is the Q_{cc} and θ is the angle between the electric field gradient and the external magnetic field.

For every I = 1 nucleus there are two lines, and the frequency distance of them is:
$\Delta\nu = 3/2\ (e^2qQ/h)\ (3\cos^2\theta - 1)$.

^2H NMR is a technique that has been used to study molecular motion in solid materials as well as to investigate molecular dynamics in organic molecules. Deuterium is an ideal nucleus to study, because its quadrupolar interactions are mainly first order, and they are sufficiently small to allow the acquisition of undistorted ^2H Pake patterns. At the same time ^2H is sensitive enough to probe molecular dynamics. Due to short T_2 relaxation times, the FID is short and the signal is lost within the first couple of μs by the deadtime of the probehead. This leads to some difficulties; however, pulse sequences such as quadrupolar echo sequences (Hahn-Echo, Solid-Echo) refocus the signal after a suitable decay to allow signal detection.[24]

The quadecho sequence (spin echo) in Figure 2-7 shows that after the 90º pulse, a dephasing time τ is allowed, during which the different magnetizations dephase. After this a 180° pulse around the y axis is applied. This way the magnetizations are transferred to the other side of the y axis within the x,y plane, but the magnetizations keep their direction of precession, and meet again after 2τ at exactly the same spot in the y direction, then dephasing starts again.[24] At this point, one begins to record the FID. The deadtime no longer has to be taken into account, since the typical values of τ are between 20 and 50 μs. Although the quadecho sequence is extremely useful for quadrupolar nuclei and their broad signals, it has the drawback that some signal intensity is lost, depending on the T_1 time.[24]

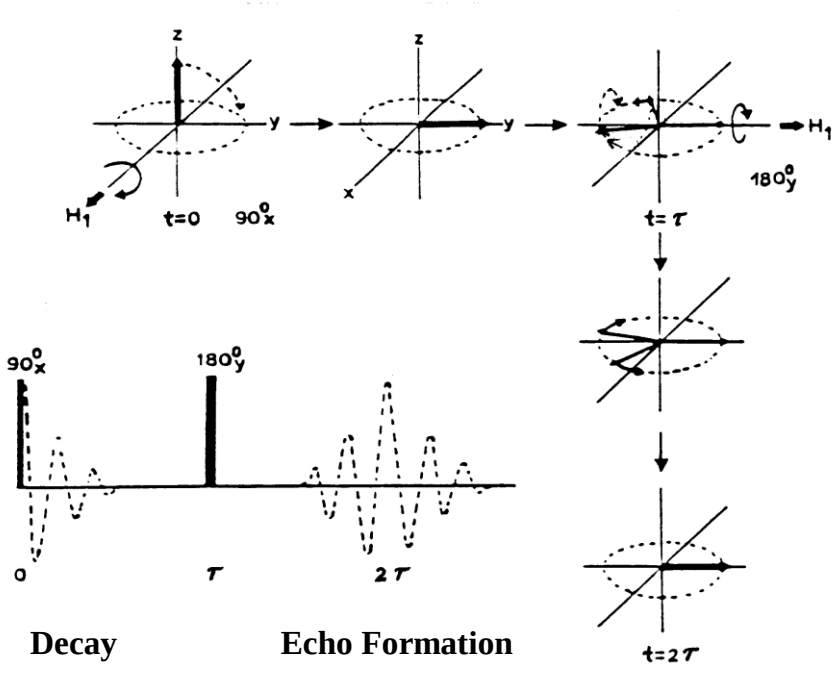

Figure 2-7. Quadrupolar echo pulse sequence.[24]

Nevertheless, deuterium (^{2}H) solid-state NMR is a powerful technique to probe the dynamics of proteins, polymers, inclusion compounds, and organic molecules adsorbed in zeolite pores or on SiO_2.[25] The lineshape for ^{2}H NMR is defined by quadrupolar interactions and is very sensitive to the mode and frequency of molecular motion. The standard ^{2}H NMR experiments commonly employed in solid-state NMR to study mobilities, besides spin echo sequences, are CP/MAS and simple high-power decoupling. CP/MAS has already been used in the group to determine the mobility of a deuterated alkyl chain in the coordination sphere of a metal complex.[26]

Because of this great analytical potential, classical solid-state NMR of the dry materials and HRMAS of slurries will be the main analytical methods for the project presented below.

2.3 Immobilization Strategies

Supported catalysts are amenable to the simplified separation and recovery of catalysts from reaction mixtures, and since the late 1960's many approaches to 'heterogenize', 'immobilize', or 'anchor' homogeneous catalysts have been published by researchers both in academia and in industry. There are mainly four distinct method-ologie to immobilize homogeneous catalysts. These are adsorption, encapsulation, covalent tethering, and binding by electrostatic interactions.[27,28]

Adsorption: Adsorption via Hydrogen Bonding

Catalysts immobilized by adsorption sometimes depend only on van der Waals interactions between the catalysts and the supports. Since this is a very weak interaction, the catalyst will readily leach into solution either due to interactions with a solvent, or because of interactions with the substrates during the catalytic reaction. But the stability of adsorbed catalysts can be improved by modifying the catalyst and support to allow hydrogen bonding to occur (Figure 2-8). Bianchini and coworkers have immobilized Rh and Ru complexes on silica gel via hydrogen bonding.[29] The supported complexes have been used for the hydrogenation of alkenes, nitriles, and α,β-unsaturated ketones. In the reduction of benzyleneacetone, the catalyst showed higher selectivity as compared to the analogous homogeneous catalyst. While the olefin moiety was reduced successfully, the carbonyl group remained intact. But the conversion of 61 % was significantly lower than the one obtained with the conventional homogeneous catalyst system (100 % conversion).

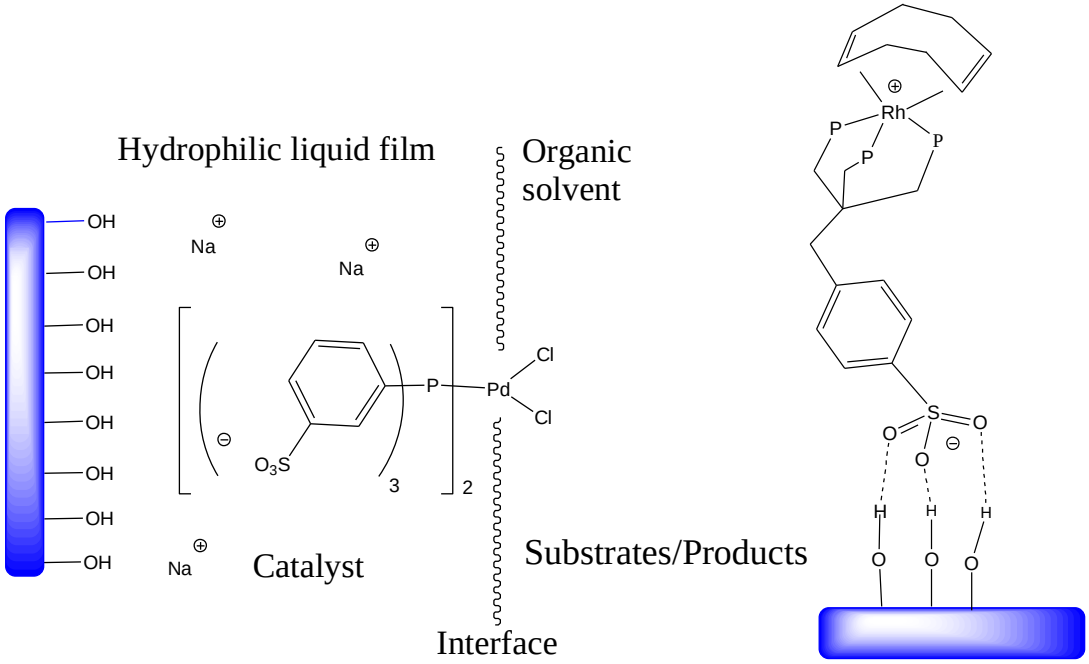

Figure 2-8. Immobilization of a Rh complex by adsorption via hydrogen bonds (right);[30] model for a supported aqueous phase (SAPC) catalyst (left).

Supported Aqueous-Phase Catalysis (SAPC)

Supported aqueous-phase catalysis (SAPC) was introduced by Davis and coworkers in 1989 as a new type of heterogeneous catalysis.[31] The key feature of this concept is to immobilize a water-soluble catalyst in a thin layer of hydrophilic liquid that is supported on a solid hydrophilic material. The catalysis is carried out in an organic layer, which is immiscible with the hydrophilic film, while the catalyst is retained on the support (Figure 2-8, right). Silica and controlled-pore glass are chosen as supports. Water and ethylene glycol are used as hydrophilic liquid phase. Sodium and lithium salts of triphenylphosphine trisulphonate (TPPTS), or guanidinium phosphine (Figure 2-9) are commonly used as water-soluble ligands to coordinate with commercially available

metal precursors. The SAPC system has successfully been applied to the Heck reaction,[32] Sonogashira reaction,[33] hydrogenation,[34] and hydroformylation.[35] The activities of the immobilized catalysts were comparable to those of the homogeneous catalysts. But recycling experiments showed that the activity decreased significantly after the first run.[36] TPPTS was oxidized during the reaction and then rendered the metal inactive.

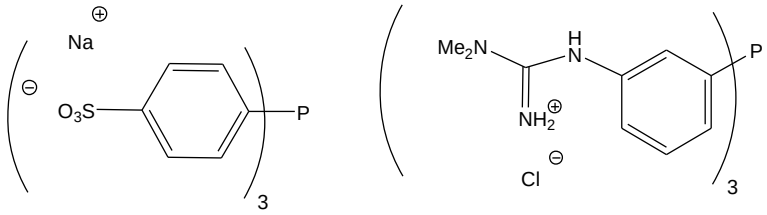

TPPTS Guanidinium phosphine

Figure 2-9. Water-soluble ligands applied in SAPC.

In the case of supported liquid-phase catalysis (SLPC), the water film on the inner surface is replaced by a solvent of low vapor pressure (e.g. phthalic acid esters).[37] The use of SLPC catalysis is generally restricted to the synthesis of low-boiling compounds.

Biphasic Fluorous Catalysis

Fluorous reversed-phase silica gel (FRPSG) has been used as the support for perfluoro-tagged catalysts.[38] The concept is based on the temperature-dependent immiscibility of perfluorinated solvents and common organic solvents. The main advantage is the solvophobicity of perfluoroalkyl tags. It results in a selective partitioning onto the fluorous reversed-phase silica gel, while untagged components possess no affinity to the fluorous phase. As a consequence, polar as well as non-polar reaction media can be used, which makes this strategy applicable to a broader range of reactions and work-up conditions. It is possible to further adjust the reactivity by release from the support during the reaction and re-adsorption after a solvent switch. Tzschucke[39] utilized FRPSG as solid support and immobilized a perfluoro-tagged Pd complex. It has successfully been applied to C-C coupling reactions and high reactivity was obtained.

Encapsulation

Avecia and Ley *et al.* co-developed the method to encapsulate palladium(0) (PdEnCat) in a polyurea framework (Figure 2-10, left) and they generated an immobilized catalyst, which has been successfully applied for hydrogenation[40] and cross-coupling reactions.[41] With the EnCat immobilization technology, no additional ligands for metal stabilization are required, since they are provided by the polymer itself. Leaching of metals was extremely low and the catalyst can be easily recovered by filtration. Jamis *et al*. studied the immobilization of a Rh-BPPM complex by entrapment

within a silica matrix by using sol-gel chemistry.[42] The immobilized catalyst has been applied to the hydrogenation reaction of sodium α-acetamidocinnimate, but the activity decreased significantly when the catalyst was re-used.

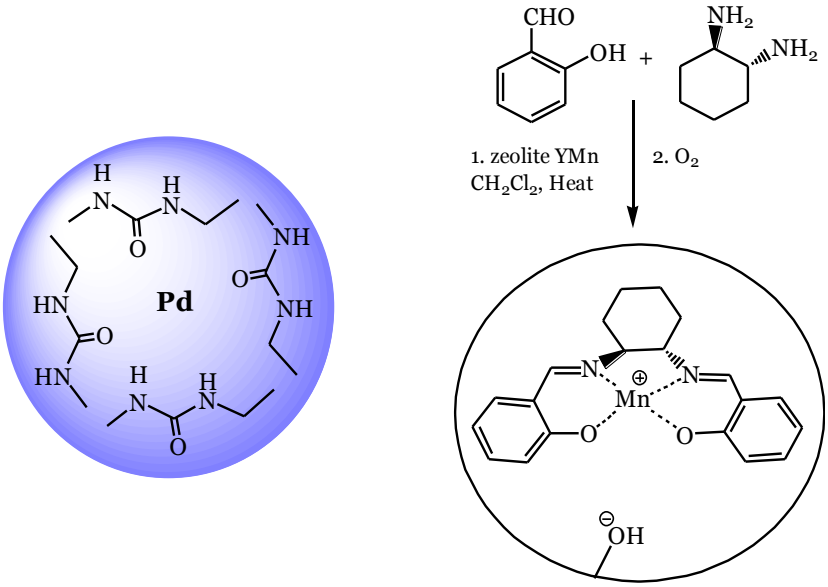

Figure 2-10. Immobilization of Pd(0) (left) and a (salen)Mn complex (right) by the encapsulation technique.

Besides building up a polymer network around a preformed catalyst, there is another method to encapsulate a catalyst. That is to generate a catalyst in well-defined cages of porous supports (Figure 2-10, right).[43] This approach is also called 'ship in a bottle'.[44]

Encapsulation is the only catalyst immobilization process, which does not require any interactions between the catalyst and the support. The technique of covalent

tethering relies on the modification of the ligand. This may influence the electronic character of the ligand, while physisorption and ion-exchange methods result in the catalyst being in close proximity to the support, which may also affect the electronic properties and the ligand conformation.

Covalent Tethering

Binding of a ligand to a solid support via covalent bonds has become the most frequently employed strategy to immobilize a homogeneous catalyst. It can be exerted either by copolymerization of functionalized ligands with suitable monomers, or by grafting functionalized ligands or metal complexes with reactive groups onto preformed supports.

In general, the support materials must be thermally, chemically, and mechanically stable during the reaction process. The active sites should be well dispersed on the support's surface and these sites should be easily accessible. Organic polymers[45] and inorganic supports[46] generally meet all those requirements and have been extensively utilized as supports.

Polymeric and Dendritic Supports

Polymeric supports revolutionized organic synthesis and catalysis throughout the twentieth century. Numerous polymeric supports, crosslinked (insoluble) and non-crosslinked (soluble) polymers, have been synthesized and applied for chemical

reactions. Functionalized polystyrenes are available as linear non-crosslinked and as crosslinked polymers. The latter ones, generally referred to as PS resins, are among the most commonly used solid supports for solid-phase organic synthesis and catalysis.[47]

The use of soluble polymers[48] as catalyst supports is another interesting way for catalyst separation. During the reaction, supported catalysts behave like homogeneous catalysts, and after the reaction, they can easily be separated by precipitation. The first examples are reported in the 1970s, when Rh-containing soluble polymers (Figure 2-11) were successfully applied as hydrogenation catalysts.[49] Since then, functionalized soluble polystyrenes,[50] polyethylene glycols,[51] polymethylmethacrylates,[52] hyperbranched polymers,[53] or polyelectrolytes[54] have been applied as soluble polymeric supports for transition metal complexes.

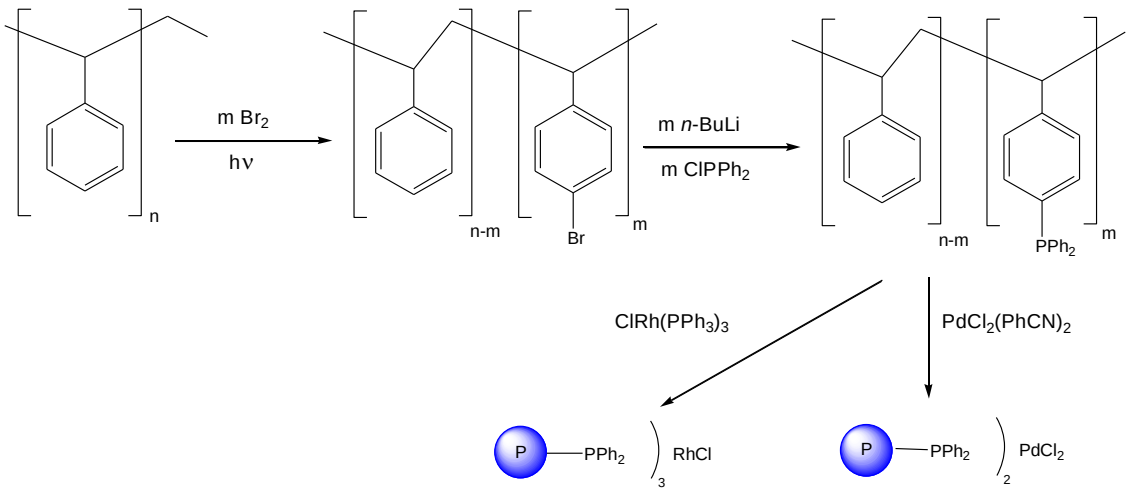

Figure 2-11. Immobilization of Rh and Pd complexes on polymer supports.

Voegtle *et al*. were the first, who brought up the idea of using dendrimers as soluble supports.[55] Compared with soluble polymers, dendrimers provide a better-defined structure. Dendritic catalysts have been applied to ruthenium-catalyzed metathesis,[56] and palladium-catalyzed reductive coupling reactions of benzene and chlorobenzene.[57] But the syntheses of the dendritic catalysts are usually tedious and expensive and, correspondingly, commercial applications of dendrimers are scarce.

2.4 Synthesis of Tetrahedral Structures

Over the years the Bluemel group has developed substantial expertise with ethoxysilane phosphine linkers.[15,57-61a] The syntheses of numerous mono-, bi-, and tridentate chelate phosphines with ethoxy groups have been optimized, and their coordination to metal centers was explored.[5] Furthermore, the reaction of ethoxysilanes with oxide supports has been studied in detail.[62]

The main insights derived from these studies, and additionally from catalysis, can be summarized as follows: The ideal linker should (a) not decompose on the surface, as phosphinoamines, for example, do,[59] (b) keep the phosphine moieties coordinating the metal complexes far enough apart from each other, so that the catalysts cannot be deactivated by dimerization or related processes,[15a,b] and (c) prevent any contact of the metal complex with the reactive silica surface, because this might lead to decomposition especially of the active form of the catalyst.[61b] While (a) and (b) can be addressed by the conventional ethoxysilane-modified phosphine linkers with alkyl chain spacers,[15,57-61a] (c) needs a fundamentally different type of linker.

Since linkers with flexible alkyl chains can "bend down" and will always allow some contact of the tethered metal complex with the surface during catalysis, the optimal linker should have a rigid backbone that excludes any bending motion.[16,6]

Organic compounds with rigid and tetrahedral scaffolds have recently become more popular.[63] The core of the molecules is typically a tetraphenylmethane or tetraphenylsilane system with a sp^3-hybridized carbon or silicon atom in the center. As an alternative, adamantyl systems were used.[64] In these systems, every second carbon atom incorporates a substituent, for which a tetrahedral structure follows. These systems are valuable for various applications, which is proven by many light-emitting organic compounds which contain tetraphenylmethane, tetraphenylsilane, or adamantyl systems. Many chromophores like vinylstilbenes,[65] triphenylethenes[65] and oxadiazolyl[66] were also bound to these structures.

Another advantage of such scaffolds arises from their rigidity: when metal complexes get in contact with reactive oxide surfaces, for example silica surfaces, they are deactivated and their lifetime is shortened. Catalyst deactivation can also occur via dimerization when the flexible phosphine linkers are immobilized with high surface coverages.[15] But with rigid scaffolds, such as tetraphosphines, bound to the surface via one, two, or three phosphonium groups (Figure 2-12), this can be prevented. These rigid linker systems lead to active catalysts which can be recycled many times.[6]

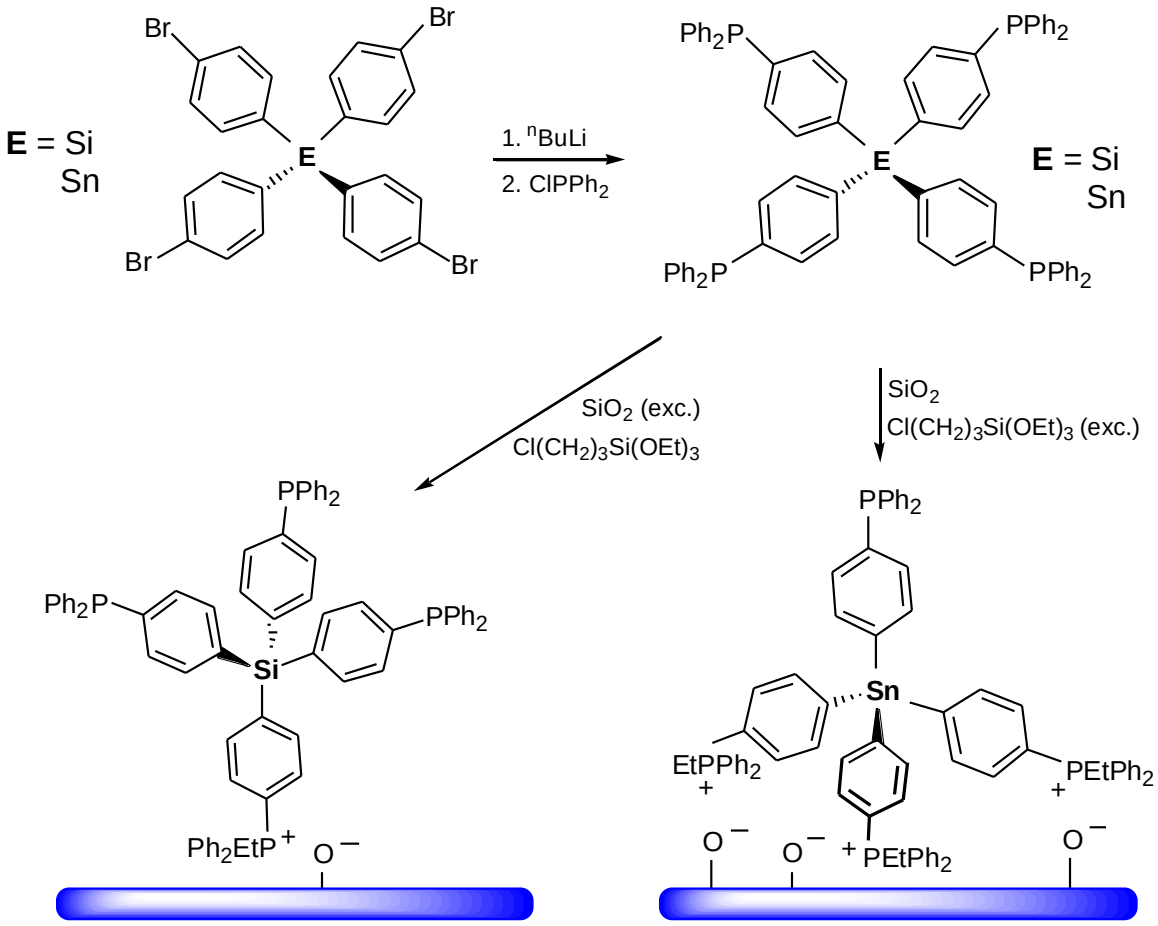

Figure 2-12. Synthesis and immobilization of tetraphosphine linker scaffolds.

There are also various applications of tetrahedral systems with rigid cores besides catalysis. In 1994 the group of Eng reported the inhibition of ceratocystis ulmi *in vitro*, the causative agent of Dutch elm disease (DED), by the tetraaryltin compounds Ph_4Sn, (m-$ClC_6H_4)_4Sn$, (m-$CH_3OC_6H_4)_4Sn$, and (m-$CH_3C_6H_4)_4Sn$.[67]

In 2009 Klein Gebbink *et al.* reported the synthesis of carbosilane dendrimers based on rigid core molecules (Figure 2-13).[68] One application for dendrimers is to function as a catalyst support in solid-phase organic synthesis (SPOS). In this process,

loss of dendritic material is often observed during filtration. Most dendrimers are not rigid globular molecules and are sensitive to some extent to shear flow, which results in diminished and variable hydrodynamic volumes under filtration conditions. One approach to improve the filtration performance of dendritic supports is to use rigid structures. These rigid dendrimers are likely to have larger hydrodynamic volumes and are less susceptible to structural deformation under shear flow.[68]

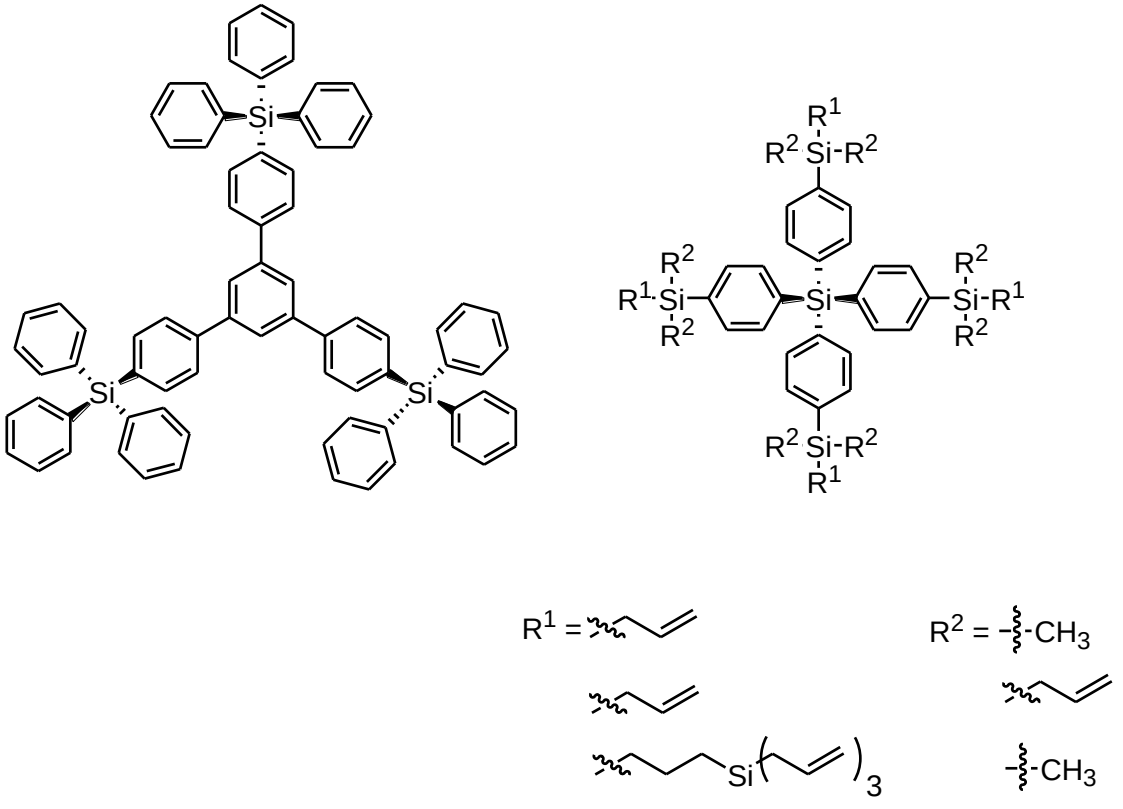

Figure 2-13. Examples of silane-containing dendrimers.[68]

In 2009 the Zhang group described the synthesis of a polyarylate with tetraphenylsilane core (Figure 2-14) via the first postpolymerization modification reaction.[69]

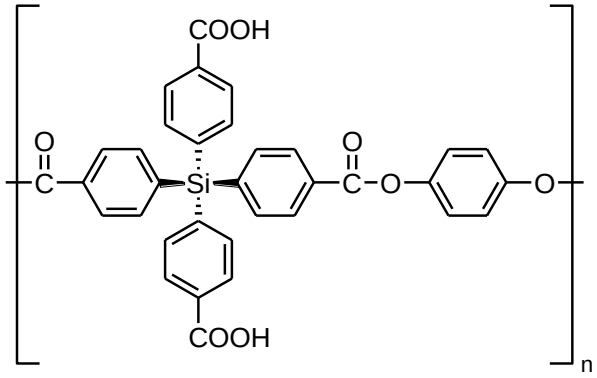

Figure 2-14. Tetraphenylsilane-containing polyarylates with well-defined functional groups.[69]

Because of the well-defined carboxylic acid groups and the rigid tetrahedral structure in each repeating unit, it seems feasible to prepare hyper-crosslinked covalent organic framework materials with permanent microporous structure and high surface area.[69]

3. EXPERIMENTAL

3.1 General Introduction

Solvents

Solvents were obtained either from the Department of Chemistry at Texas A&M University or from VWR. The removal of oxygen and dehydration of the solvents was carried out according to standard procedures. Toluene, THF, Et_2O, and pentane were dried by refluxing over Na in a nitrogen atmosphere for several days and stored over molecular sieves under a nitrogen atmosphere in Schlenk flasks.

Methods

All syntheses and manipulations were carried out on a double–manifold Schlenk vacuum line under a nitrogen atmosphere. The inert gas, nitrogen, was purified with gas purifying columns filled (a) with catalyst [R 3-11] (5x3 mm) from BASF and (b) with molecular sieves (3 Å) from Roth. For an air-tight seal of the glass joints the teflon grease Barrierta L 55/3 HV by the company Klüber Lubrication and silicon high vacuum grease by the company Wacker was used.

SiO_2

The silica 40 (40 Å average pore diameter, 750 m^2/g specific surface area, 0.063 - 0.2 mm average particle diameter) used for the immobilization reactions was

purchased from the company Merck. The silica was heated for one week at a vacuum line under oil pump vacuum at 500°C to remove adsorbed water and to condense most Si-OH groups on the silica surface. The dried silica was stored under nitrogen in a Schlenk flask.

Melting Points

Samples were measured in a glass capillary with the melting point instrument MP A 100 Opti Melt of the company Stanford Research Systems.

NMR Measurements

^{1}H NMR spectra were measured with a Varian Inova 500. As solvents and internal standards, acetone-d_6, benzene-d_6, $CDCl_3$, and CD_2Cl_2 were used. The spectra could be interpreted first order. The following abbreviations were used: s = singlet, d = doublet, t = triplet, q = quartet, dd = double doublet, etc. and m = multiplet. ^{13}C NMR spectra were measured with a Varian Inova 500. All ^{13}C NMR spectra were measured with broadband proton decoupling. ^{31}P NMR spectra were measured with a Varian Inova 500. As an external standard in a glass capillary, centered in the middle of the 5 mm NMR tube, neat $ClPPh_2$ with a chemical shift of 81.92 ppm was used. For the leaching studies, 0.5 ml of a 0.07 M solution of **3-4** was placed in a NMR tube along with the external standard in the capillary. The ^{31}P NMR was measured and the integral of the phosphonium salt was compared to that of the external standard and was regarded

as the maximum amount of leaching. From this integral all other concentrations could be calculated. ^{119}Sn NMR spectra were measured with a Varian Unity Inova 400 FT NMR.

Solid-State NMR

^{31}P and ^{2}H solid-state NMR spectra were measured with a Bruker Avance DSX-400 solid-state NMR spectrometer. For all 7 mm ^{31}P measurements, AMP with a chemical shift of δ = 1.3 ppm was used as an external reference and for 4 mm ^{31}P measurements, ADP with a chemical shift of δ = 0.81 ppm. ^{31}P MAS was measured with ^{1}H high-power decoupling if not stated otherwise, and with a delay of 10 seconds. For ^{31}P CP/MAS measurements, the contact time was 1 to 5 ms. The rotational frequency for 7 mm ^{31}P measurements was 4 kHz, if not stated otherwise, and 9 kHz for 4 mm ^{31}P NMR measurements. For 7 mm ^{2}H measurements PMMA was used as the standard. All ^{2}H NMR spectra were measured with a Hahn-echo pulse program unless stated otherwise.

Surface Area

The specific surface coverage Θ is given as the number of immobilized molecules per 100 nm^2 of surface.

3.2 Reagents and Solvents

All listed reagents and solvents were obtained from the stockroom of the Department of Chemistry at Texas A&M University or from the stock of the group, except:

^{n}BuLi (1.6 M in n-hexane)	Aldrich
^{n}BuLi (2.5 M in n-hexane)	Aldrich
Chlorodiphenylphosphine	TCI
3-Chloropropyltriethoxysilane	Aldrich
1,4-Dibromobenzene	Aldrich
Tintetrachloride	Alfa Aesar
Triphenylphosphine	Aldrich
Bromoethane	Alfa Aesar
Iodomethane	Alfa Aesar
Iodomethane-d_3	Aldrich
Bromobenzene-d_5	Sigma

3.3 Synthesis of Ligands

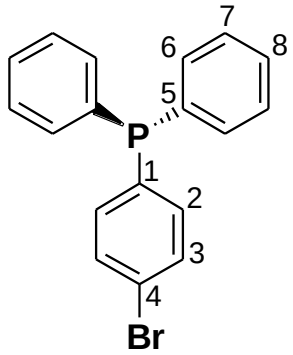

3-1
$C_{18}H_{14}BrP$
Mol. Wt.: 341.180 $^{g}/_{mol}$

Synthesis of 4-bromophenyldiphenylphosphine (3-1)

A solution of ^{n}BuLi (1.6 M, 15.0 mL, 24.0 mmol) was added dropwise to a solution of 1,4-dibromobenzene (5.66 g, 24.0 mmol) and Et_2O (100 mL) at -50°C. The mixture was warmed up to ambient temperature, stirred for 15 mins, cooled down to 50°C, and $ClPPh_2$ (4.41 mL, 24.0 mmol) was added dropwise. The mixture was then stirred overnight at RT. The solvent was then removed *in vacuo*. The product was extracted from the residue with toluene (3×20 mL), and the solvent was removed *in vacuo* to yield a white powder of **3-1** (7.66 g, 22.4 mmol) in 93.5 % yield. $^{31}P\{^{1}H\}$ NMR (acetone-d_6, 202.28 MHz): δ (ppm) = -6.73 (s). $^{13}C\{^{1}H\}$ NMR (acetone-d_6, 125.66 MHz): δ (ppm) = 137.87 (d, $^{1}J(^{31}P\text{-}^{13}C)$ = 12.6 Hz, C_1), 137.45 (d, $^{1}J(^{31}P\text{-}^{13}C)$ = 10.4 Hz, C_5), 136.09 (d, $^{2}J(^{31}P\text{-}^{13}C)$ =20.2 Hz, C_2), 134.38 (d, $^{2}J(^{31}P\text{-}^{13}C)$ = 19.9 Hz, C_6), 132.50

(d, $^{3}J(^{31}P\text{-}^{13}C)$ = 6.8 Hz, C_3), 129.93 (s, C_8), 129.58 (d, $^{3}J(^{31}P\text{-}^{13}C)$ = 7.1 Hz ,C_7), 123.78 (s, C_4).

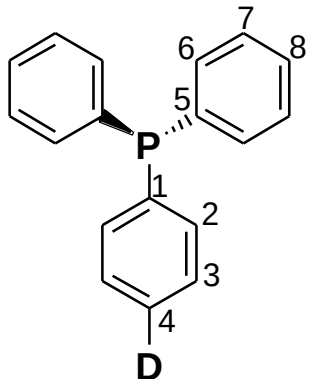

3-2
$C_{18}H_{14}DP$
Mol. Wt.: 263.29 $^{g}/_{mol}$

Synthesis of (p-Deuterophenyl)diphenylphosphine (3-2)

A solution of ^{n}BuLi (1.6 M, 2.44 mL, 3.91 mmol) was added dropwise to a solution of **3-1** (1.34 g, 3.91 mmol) and Et_2O (300 mL) at -78°C. The mixture was left to stir at -78°C for 2 h and then slowly warmed up to ambient temperature. The yellow solution was then quenched with 10 mL of D_2O. After 2 h of stirring, the solution was quenched with NH_4Cl. The organic layer was collected and dried over Na_2SO_4. Then the solvent was removed *in vacuo* to yield **3-2** (720 mg, 2.74 mmol) in 69.9 % yield. $^{13}C\{^{1}H\}$ NMR ($CDCl_3$, 125.66 MHz): δ (ppm) = 138.16 (d, ^{1}J ($^{31}P\text{-}^{13}C$) = 11.6 Hz, C_1/C_5), 134.36 (d, $^{2}J(^{31}P\text{-}^{13}C)$ = 19.6 Hz, C_2/C_6), 129.65 (s, C_8), 129.42 (d, $^{3}J(^{31}P\text{-}^{13}C)$ =

6.8 Hz , C_7), 129.32 (d, ^3J (^{31}P-^{13}C) = 6.8Hz, C_3). ^2H NMR (acetone-d_6, 61.33 MHz): δ (ppm) = 7.40 (s, D). $^{31}P\{^1H\}$ NMR ($CDCl_3$, 202.28 MHz): δ (ppm) = -5.73 (s).

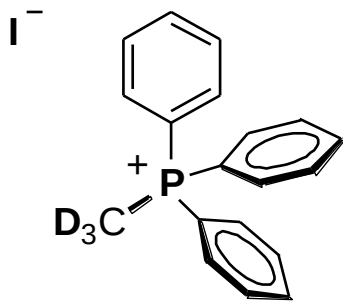

3-3
$C_{19}H_{15}D_3IP$
Mol. Wt.: 407.243 $^g/_{mol}$

Synthesis of Methyltriphenylphosphoniumiodide-d_3 (3-3)

Triphenylphosphine (272 mg, 1.04 mmol) was dissolved in toluene (5 mL) in a Schlenk flask under a N_2 atmosphere. After adding MeI-d_3 (233 mg, 1.61 mmol) via syringe the reaction mixture was stirred overnight at RT. The solvent was removed *in vacuo* and the residue was washed with pentane (2×5 mL) to give **3-3** (410 mg, 1.00 mmol) as a white powder with a yield of 97 %. $^1H\{^{31}P\}$ NMR ($CDCl_3$, 499.70 MHz): δ (ppm) = 7.80 (t, $^3J(^1H$-$^1H)$ = 7.2 Hz), 3H, H_{para}), 7.73 (d, $^3J(^1H$-$^1H)$ = 7.2 Hz), 6H, H_{ortho}), 7.68 (dd, $^3J(^1H$-$^1H)$ = 7.4 Hz), 6H, H_{meta}). $^{13}C\{^{31}P,^1H\}$ NMR ($CDCl_3$, 125.66 MHz): δ (ppm) = 135.31 (C_{para}), 133.34 (C_{ortho}), 130.59 (C_{meta}), 118.76 (C_{ipso}), 10.98 (sept., ^1J (^{13}C-^2H) = 20 Hz), CD_3). ^2H NMR (acetone-d_6, 61.33 MHz): δ (ppm) = 3.58 (s,

CD_3). $^{31}P\{^1H\}$ NMR ($CDCl_3$, 202.28 MHz): δ (ppm) = 21.34 (s). ^{31}P MAS (ν_{rot}= 4 kHz): δ (ppm) = 20.05 (s) (isotropic line).

Methyltriphenylphosphonium iodide (3-4) was prepared as described above with 100% yield. **Methyltriphenylphosphonium bromide (3-5)**, **Ethyltriphenylphosphonium chloride (3-6)**, **Ethyltriphenylphosphonium bromide (3-7)**, **Ethyltriphenylphosphonium iodide (3-8)**, and **Ethyltriphenylphosphonium tetrafluoroborate (3-9)** were all obtained from a previous group member.

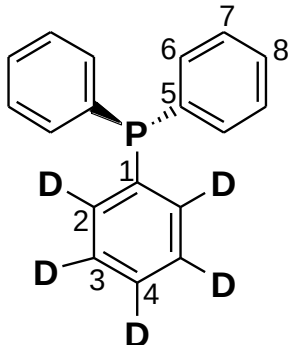

3-10
$C_{18}H_{10}D_5P$
Mo. Wt.: 267.318 g/mol

Synthesis of Diphenyl(pentadeuterophenyl)phosphine (3-10)

A solution of ^{n}BuLi (8.90 mL, 14.2 mmol) was added dropwise to a stirred solution of bromobenzene-d_5 (1.50 mL, 14.2 mmol) in 50 mL of Et_2O at -78°C. The solution was slowly warmed up to RT and then stirred for 2 h. The transparent solution was afterwards cooled down again to -78°C. Then $ClPPh_2$ (2.56 mL, 14.2 mmol) was added dropwise to the solution. The reaction mixture was stirred at room temperature

overnight and then filtered to remove the lithiumchloride. The solvent was removed *in vacuo* and the final product was crystallized in acetone to give **3-10** with a yield of 80.1%. $^{1}H\{^{31}P\}$ NMR (acetone-d_6, 500.13 MHz): δ (ppm) 7.39-7.37 (m, 6H, H_{meta}, H_{para}), 7.30-7.27 (m, 4H, H_{ortho}). $^{13}C\{^{31}P,^{1}H\}$ NMR (acetone-d_6, 125.66 MHz): δ (ppm) = 138.22 (d, ^{1}J (^{31}P-^{13}C) = 11.6 Hz, C_5), 134.38 (d, ^{2}J(^{31}P-^{13}C) = 19.7 Hz, C_6), 129.45 (d, ^{3}J(^{31}P-^{13}C) = 6.8 Hz , C_7), 129.68 (s, C_8),). $^{31}P\{^{1}H\}$ NMR (acetone-d_6, 202.28 MHz): δ (ppm) = -6.17 (s). ^{2}H NMR (acetone-d_6, 46.07 MHz): δ (ppm) = 7.98 (s)

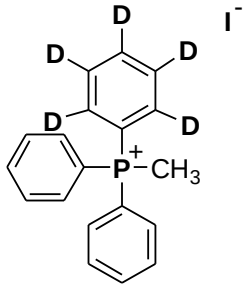

3-11
$C_{19}H_{13}D_5P$
Mol.Wt.: 282.141 $^{g}/_{mol}$

Synthesis of Methyldiphenyl(pentadeuterophenyl)phosphonium iodide (3-11)

Diphenyl(pentadeuterophenyl)phosphine (209 mg, 0.78 mmol) was dissolved in toluene (10 mL) in a Schlenk flask under a N_2 atmosphere. Then MeI (110 mg, 0.77 mmol) was added via syringe. Then the reaction mixture was stirred overnight at RT. The solvent was removed *in vacuo* and the residue was washed with pentane (2×5 mL)

to give **3-11** (750 mg, 2.66 mmol) as a white powder with a yield of 96%. $^{31}P\{^{1}H\}$ NMR (acetone-d_6 , 202.28 MHz): δ (ppm) = 22.18 (s).

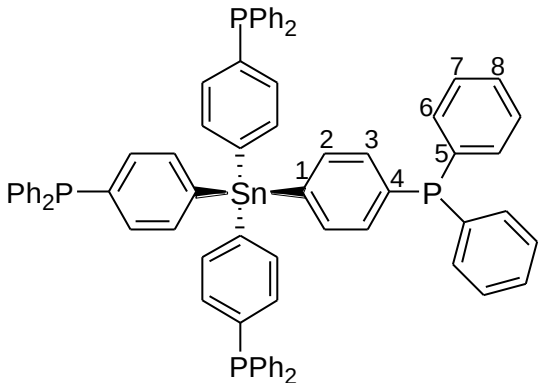

3-12
$C_{72}H_{56}P_4Sn$
Mol.Wt.: 1163.820 $^{g}/_{mol}$

Synthesis of Tetrakis(4-diphenylphosphanylphenyl)stannane (3-12)

^{n}BuLi (1.87 mL, 4.69 mmol in 2.5 M hexane) was added dropwise to a stirred solution of **3-1** (1.59 g, 4.69 mmol) in Et_2O (400 mL) at -60°C. The mixture was slowly warmed up to RT and then stirred over a span of 2 h. Then the mixture was cooled down to -60°C and $SnCl_4$ (0.13 mL, 1.17 mmol, 0.29 g) was added dropwise. After warming up to ambient temperature and stirring overnight, the solvent was removed *in vacuo*. **3-12** was extracted from the residue with toluene (3×20 mL), and the solvent was removed *in vacuo*. After recrystallization in toluene, 3483 mg (2.99 mmol, 43.1 %) of **3-12** was obtained. $^{31}P\{^{1}H\}$ NMR (C_6D_6, 202.28 MHz): δ (ppm) = -5.13 (s). $^{13}C\{^{1}H\}$ NMR (C_6D_6,

125.66 MHz): δ (ppm) = 139.52 (d, ^{1}J (^{31}P-^{13}C) = 12.5 Hz, C_4), 138.31 (s, C_1), 137.64 (d, ^{1}J(^{31}P-^{13}C) = 11.9 Hz, C_5), 137.60 (d, ^{3}J (^{31}P-^{13}C) = 6.2Hz, C_2), 134.28 (d, ^{2}J(^{31}P-^{13}C) = 19.7 Hz, C_6), 134.13 (d, ^{2}J(^{31}P-^{13}C) = 18.0 Hz, C_3), 128.98 (s, C_8), 128.85 (d, ^{3}J(^{31}P-^{13}C) = 6.9 Hz, C_7).

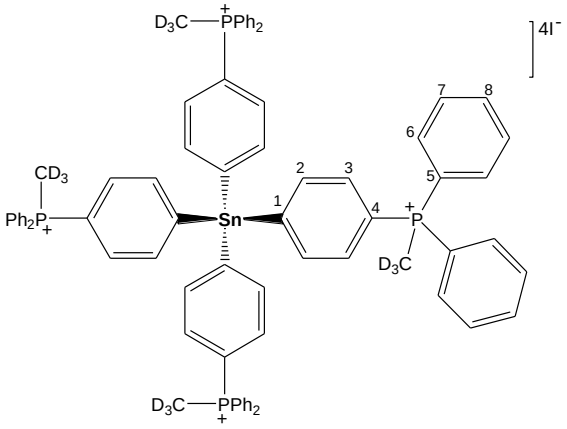

3-13
$C_{76}H_{56}D_{12}I_4P_4Sn$
Mol. Wt.: 1743.021 $^{g}/_{mol}$

Synthesis of Tetrakis[4-(diphenylmethylphosphoniumiodide)-phenyl]stannane-d_{12} (3-13)

3-12 (1.43 g, 1.22 mmol) was dissolved in CH_2Cl_2 and reacted with iodomethane-d_3 (0.60 mL, 9.64 mmol) to yield **3-13** as a yellow powder in 75% yield after washing with pentane. $^{1}H\{^{31}P\}$ NMR (CD_2Cl_2, 499.70 MHz): δ (ppm) =7.86-7.80

(m, 16H, $H_{2,3}$) 7.76 -7.68 (m, 40H, $H_{6,7,8}$). $^{13}C\{^{31}P,^{1}H\}$ NMR ($CDCl_3$, 125.66 MHz): δ (ppm) = 144.48 (C_1), 138.75 (C_2), 135.13 (C_8), 133.31(C_6), 133.19 (C_3), 130.33 (C_7), 120.77 (C_4), 118.29 (C_5). $^{13}C\{^{1}H\}$ NMR (CD_2Cl_2, 125.66 MHz): δ (ppm) = 144.48 (d, ^{4}J (^{31}P-^{13}C) = 2.5 Hz, C_1), 138.75 (d, ^{3}J (^{31}P-^{13}C) = 12.1 Hz, C_2), 135.13 (d, ^{4}J (^{31}P-^{13}C) = 2.5 Hz, C_8), 133.31 (d, ^{2}J (^{31}P-^{13}C) = 10.7 Hz, C_6), 133.19 (d, ^{2}J (^{31}P-^{13}C) = 10.8 Hz, C_3) 130.33 (d, ^{3}J (^{31}P-^{13}C) = 12.8 Hz, C_7), 120.77 (d, ^{1}J(^{31}P-^{13}C) = 87.6 Hz, C_4), 118.29 (d, ^{1}J(^{31}P-^{13}C) = 88.4 Hz ,C_5). $^{31}P\{^{1}H\}$ NMR (CD_2Cl_2, 202.28 MHz): δ (ppm) = 21.26 (s). ^{119}Sn NMR (CD_2Cl_2,148.97 MHz)): δ (ppm) = -137.00 (quint, ^{5}J (^{119}Sn-^{31}P) = 19.7 Hz). ^{2}H NMR (CH_2Cl_2, 61.33 MHz) δ (ppm) = 3.22. Melting range: 88-99°C.

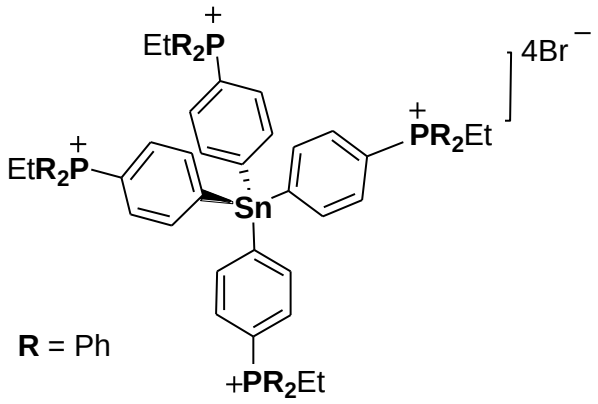

3-14
$C_{81}H_{80}Br_4P_4Sn$
Mol. Wt.: 1615.724 $^{g}/_{mol}$

Synthesis of Tetrakis[4-(diphenylethylphosphoniumiodide)phenyl]stannane (3-14)

Bromoethane (10.3 g, 94.4 mmol) was added to a solution of **3-12** (1.00 g, 0.86 mmol) dissolved in CH_2Cl_2 and left to stir for five days to yield **3-14** after washing with pentane. The exact percent yield could not be calculated because of impurities. $^{31}P\{^{1}H\}$ NMR (CD_2Cl_2, 202.28 MHz): δ (ppm) = 26.07 (s). ^{119}Sn NMR (CD_2Cl_2,148.97 MHz): δ (ppm) = -141.57 (quint, ^{5}J (^{119}Sn-^{31}P) = 19.2 Hz).

3.4 Immobilization

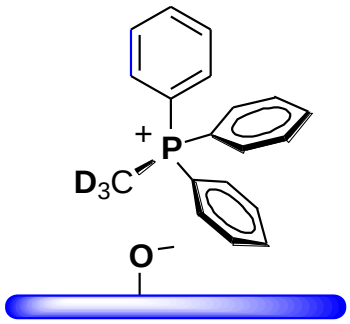

3-3i

Immobilized Methyltriphenylphosphoniumiodide-d_3 (3-3i)

3-3 (126 mg, 0.45 mmol) was dissolved in CH_2Cl_2 (24.0 mL). In a separate flask, silica (723 mg) was weighed in and suspended in CH_2Cl_2. The phosphonium salt solution was then added to the silica slurry under a N_2 atmosphere. The mixture was then stirred overnight at RT. Then the solvent was removed *in vacuo* after which the SiO_2 was washed three times with toluene, 30.0 mL each, and dried *in vacuo*. Surface

Coverage: 29 particles/100 nm^2. No ^{31}P NMR signal was observed in the supernatant. Calculations of the maximum area occupied by the phosphonium salt as a monolayer was found to be 30 particles/100 nm^2. These calculations were based on the bond lengths from the X-Ray structure. In addition, first the phosphonium salt was adsorbed with 114 particles/100 nm^2. The modified SiO_2 was then washed several times, 15 minutes each, until no ^{31}P signal was observed any more in the supernatant. The surface coverage at this point was determined by weighing the difference of the flasks with supernatant after removal of the solvent. 30 particles/100 nm^2 was the surface coverage where no more leaching was observed using this procedure. ^{31}P MAS NMR (ν_{rot} = 4 kHz): δ (ppm) = 21.68 (s) (isotropic line). All other phosphonium salts were immobilized accordingly to give an isotropic line (Table 3-1).

Table 3-1. The ^{31}P MAS NMR chemical shifts for **3-4i** to **3-9i** (ν_{rot} = 4 kHz, **Θ** corresponds to 30 particles/100 nm^2).

Phosphonium Salt	Immobilized Phosphonium salt	$\delta(^{31}P)$ [ppm]
$[MePPh_3]^+I^-$	**3-4i**	20.9
$[MePPh_3]^+Br^-$	**3-5i**	19.9
$[EtPPh_3P]^+Cl^-$	**3-6i**	25.1
$[EtPPh_3P]^+Br^-$	**3-7i**	25.0
$[EtPPh_3P]^+I^-$	**3-8i**	24.4

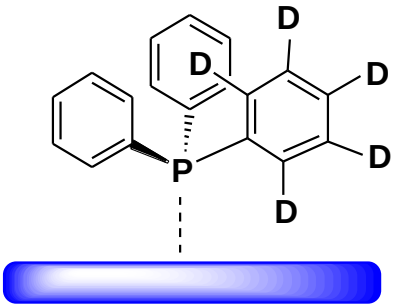

3-10a

Adsorbed Diphenyl(pentadeuterophenyl)phosphine (3-10a)

3-10 (79.0 mg, 0.29 mmol) was dissolved in pentane (50 mL). The resulting solution was then added to dry SiO_2 (229 mg). The mixture was left to stir for 10 h at RT. The supernatant was removed *in vacuo*, after which the SiO_2 was dried for 6 h *in vacuo*. Surface Coverage: 114 particles/100 nm^2.

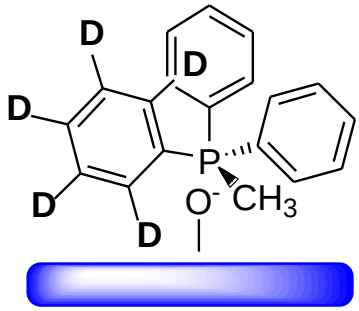

3-11i

Immobilized Methyldiphenyl(pentadeuterophenyl)phosphonium iodide (3-11i)

3-11 (105 mg, 0.39 mmol) was dissolved in CH_2Cl_2 (20 mL). In a separate flask, SiO_2 (1.04 g) was weighed in and sufficient CH_2Cl_2 was added to make a slurry. The phosphonium salt solution was then added to the silica slurry under a N_2 atmosphere. The mixture was stirred overnight at RT, then the supernatant decanted and the SiO_2 was washed with toluene (3×20 mL). The SiO_2 was then dried *in vacuo*. Surface Coverage: 30 particles/100 nm^2. No ^{31}P signal was observed in the supernatant.^{31}P MAS NMR: δ (ppm) = 22.0.

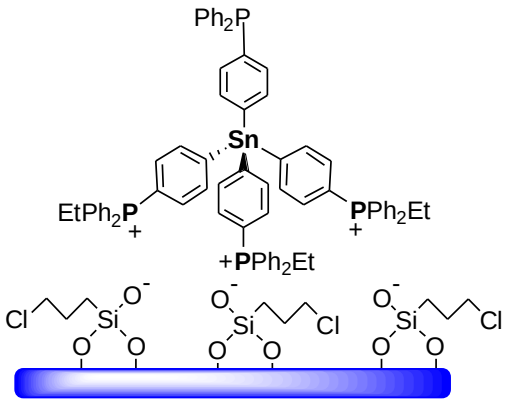

3-12i

Immobilized Tetrakis(4-diphenylphosphanylphenyl)stannane (3-12i)

To a suspension of 1.14 g of SiO_2 in 10 mL of toluene a solution of the tetraphosphine **3-12** (1.0 eq., 65.0 mg, 0.06 mmol) in 50 mL of toluene was added. Then $Cl(CH_2)_3Si(OEt)_3$ (100 eq, 1.41 g, 5.87 mmol) was added. The mixture was heated to 90°C and stirred for 5 to 7 days. After cooling down to ambient temperature, the solvent was decanted and the SiO_2 was washed with toluene (3×20 mL). The SiO_2 was then dried *in vacuo*. ^{31}P NMR of supernatant showed no signs of leaching. Surface Coverage: 4 particles/100 nm^2. ^{31}P MAS NMR: δ (ppm) = 22.2 ($–PPh_2Et^+$), -5.9 ($-PPh_2$).

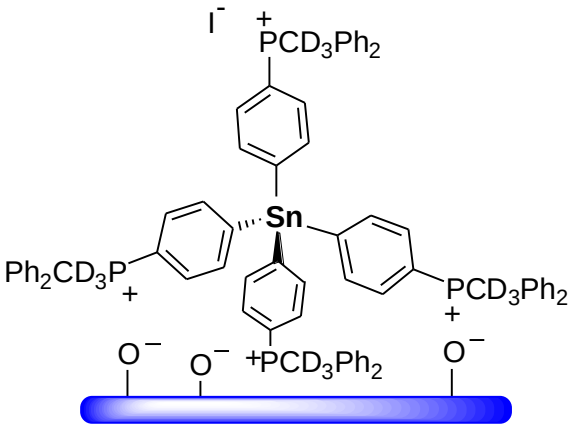

3-13i

Immobilized Tetrakis[4-(diphenylethylphosphoniumiodide)phenyl]stannane (3-13i)

3-13 (612 mg, 0.35 mmol) was dissolved in CH_2Cl_2 (20 mL). In a separate flask, SiO_2 (1.41 g) was weighed in and sufficient CH_2Cl_2 was added to make a slurry. The phosphonium salt solution was then added to the silica slurry under a N_2 atmosphere. The mixture was stirred overnight at RT, then the supernatant was removed in vacuo and the SiO_2 was washed with toluene (2× 30 mL). The SiO_2 was then dried *in vacuo*. Surface Coverage: 20 particles/100 nm^2. ^{31}P MAS NMR: δ (ppm) = 20.9.

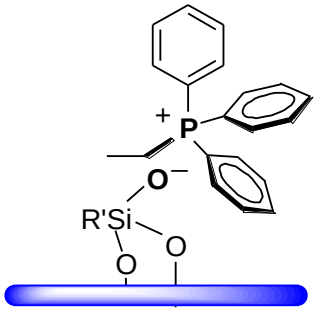

3-15i

Immobilized surface-generated phosphonium salt 3-15i

To a suspension of 4.03 g of SiO_2 in 10 mL of toluene a solution of PPh_3 (378 mg, 1.44 mmol) in 50 mL of toluene was added. Then $Cl(CH_2)_3Si(OEt)_3$ (50 eq, 17.7 g, 73.4 mmol) was added. The mixture was heated to 90°C and stirred for 4 days. After cooling down to ambient temperature, the supernatant was removed *in vacuo* and the SiO_2 was washed with toluene (3×20 mL). The SiO_2 was then dried *in vacuo*. The surface coverage was determined by assuming that all of PPh_3 added were bound to the SiO_2 surface and ^{31}P NMR of supernatant showed no signs of leaching. Surface Coverage: 29 particles/100 nm^2. ^{31}P MAS NMR**:** δ (ppm) = 21.3.

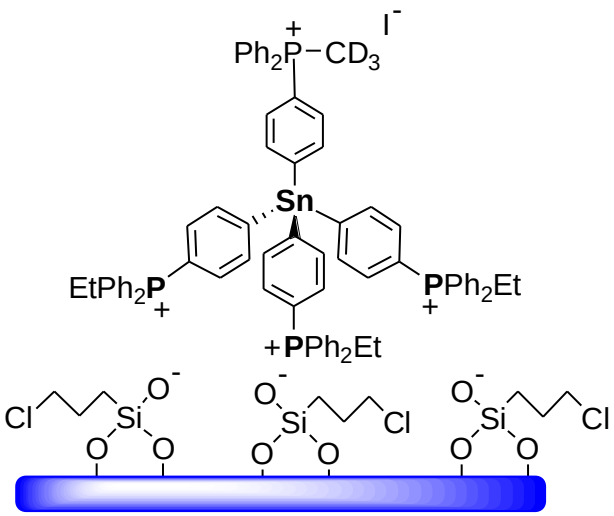

3-16i

Immobilized 3-16i

3-12i was reacted with an excess of CD_3I in CH_2Cl_2. The mixture was then stirred overnight at RT. Then the supernatant was decanted and the SiO_2 was dried *in vacuo*. ^{31}P MAS NMR: δ (ppm) = 21.7.

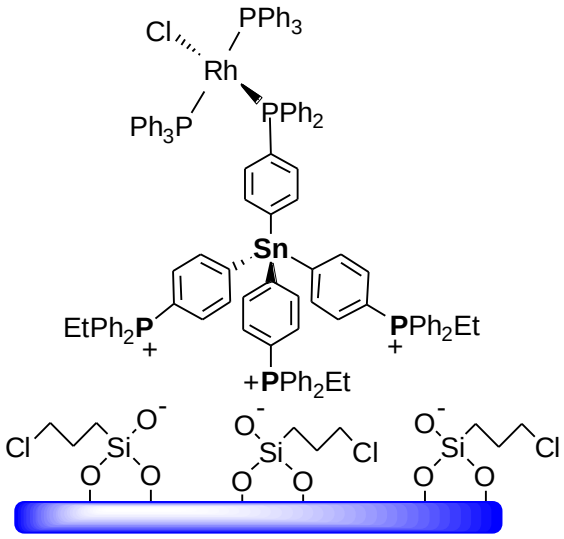

3-17i

Coordination of $ClRh(PPh_3)_3$ to 3-12i to produce 3-17i.

0.88 g of the immobilized **3-12i** was placed in a Schlenk flask and stirred with 10 mL of toluene. To this suspension, a solution of Wilkinson's catalyst $ClRh(PPh_3)_3$ (32.00 mg, 0.04 mmol) in 10 mL of toluene was added. After stirring over night at ambient temperature, the silica turned dark orange. After washing with toluene (3x20 mL) until the supernatant was colorless, the solvent was removed in vacuo, and the silica was dried at the vacuum line, where it then turned slightly orange. ^{31}P CP/MAS NMR: δ = 35.0 (s, $-PPh_2RhCl(\underline{P}Ph_3)_2$), 22.9 (s, $-\underline{P}Ph_2Et^+$).

3.5 Leaching

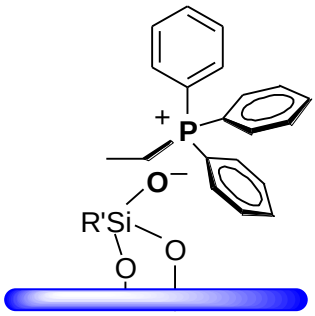

3-15i

(1.00 g) of the immobilized species **3-15i** was placed in a Schlenk flask and stirred with an acetic acid solution in acetone (5 mL, 1M) overnight. Then 0.50 mL of the supernatant was removed and placed in an NMR tube equipped with a capillary containing the reference. The ^{31}P NMR showed no leaching.

(1.00 g) of the immobilized species **3-15i** was placed in a Schlenk flask and stirred with a NaOH solution in MeOH (5 mL, 1M) overnight. Then 0.50 mL of the supernatant was removed and placed in an NMR tube equipped with an internal standard. The ^{31}P NMR was measured and the integral of the phosphonium salt was compared to that of the external standard. ^{31}P NMR showed no leaching.

4. RESULTS AND DISCUSSION

4.1 Mobility Studies

As mentioned before, our most promising system is the new generation of rigid linkers, in particular **3-12i**. The catalysts immobilized by this linker have prolonged lifetimes as compared to catalysts tethered with flexible alkyl chain linkers.[14] They can be recycled many more times.[6] Therefore it is of interest to study how these linkers bind to the surface. Questions such as: are they fixed on the surface, can they jump from site to site, and also how they react in a "real life" scenario, for example in the presence of a solvent, are of interest. However, because of the difficult synthesis/purification, and also to avoid any complications, we decided to start our studies on model compounds (**3-3**, **3-10**, **3-11)**.

The arylphosphine **3-2** was the first deuterated phosphine that was synthesized and immobilized on SiO_2. However, due to the small number of deuterium atoms in the molecule, it took several days to obtain a good signal to noise ratio, and thus a decent spectrum of the polycrystalline material (Figure 4-1).

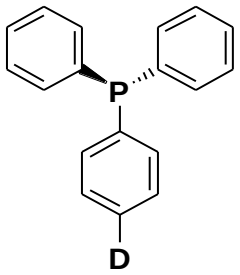

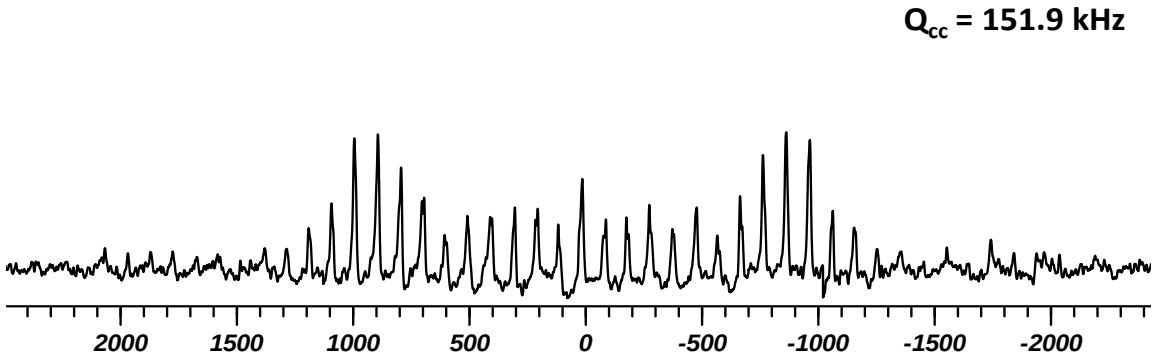

Figure 4-1. ^{2}H MAS NMR of polycrystalline **3-2** with ^{1}H high-power decoupling at 6 kHz.

This drawback then focused our attention on **3-10** and **3-11** that consisted of sufficient deuterium to be monitored in a reasonable time (Scheme 4-1).

Scheme 4-1. Adsorbed diphenyl(pentadeuterophenyl)phosphine **3-10a** and **3-11i**, bound by electrostatic interactions.

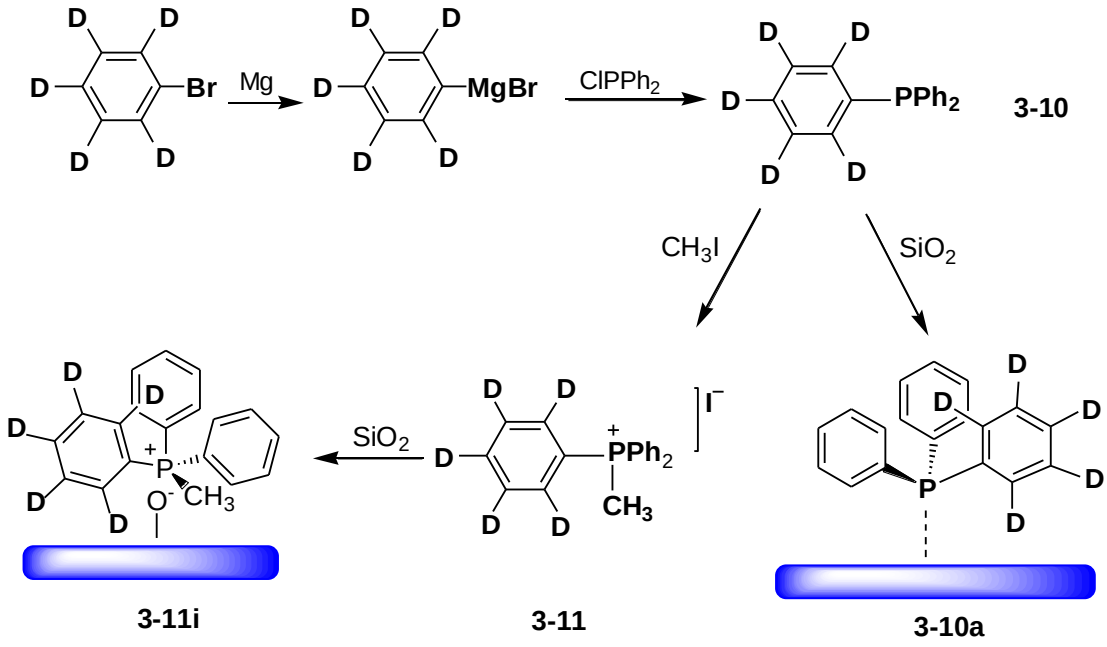

Polycrystalline **3-10** showed a quadrupolar coupling constant (Q_{cc}) of 161.3 kHz, which is indicative of the absence of motion (Figure 4-2). Similarly, polycrystalline **3-11** displayed an averaged Q_{cc} of approximately 151 kHz (Figure 4-3), which is also due to the absence of rapid motion.

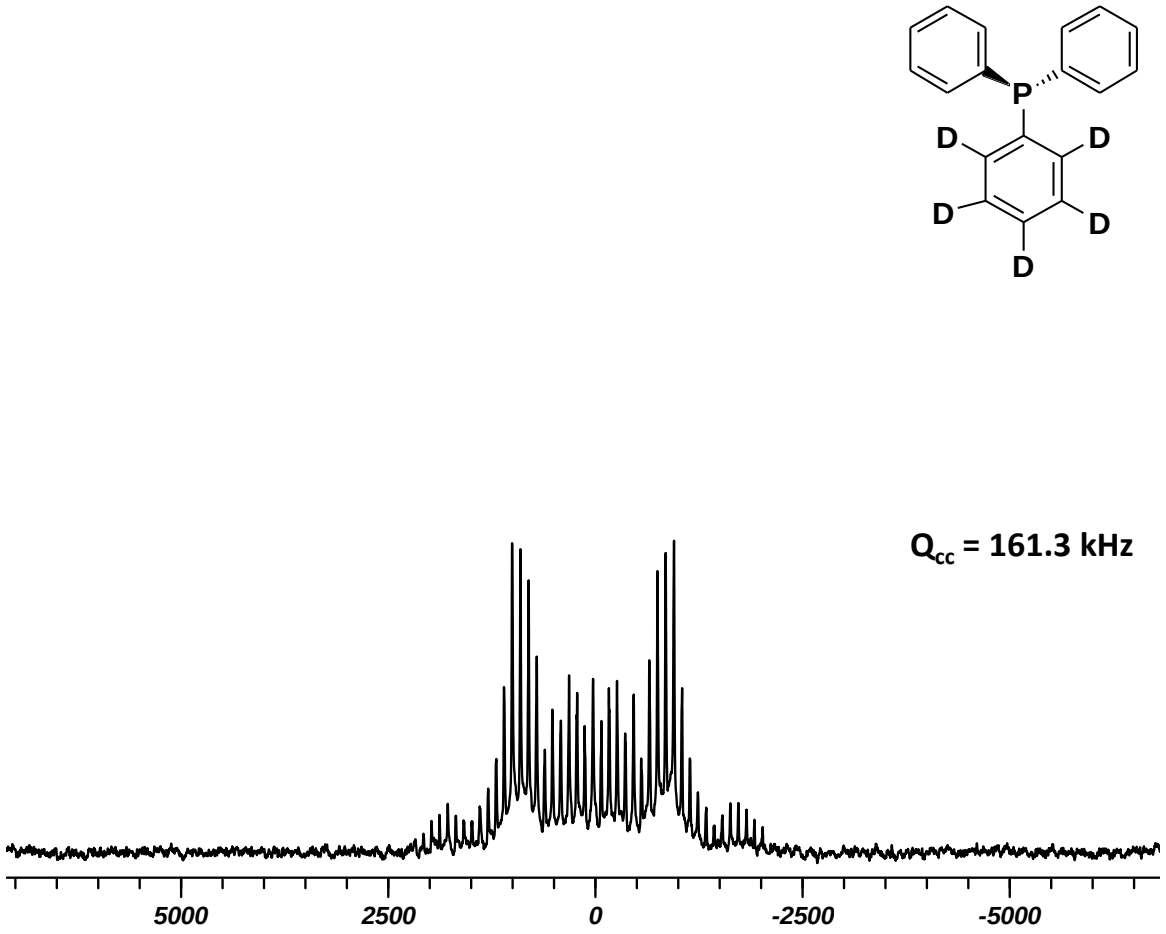

Figure 4-2. ^{2}H MAS NMR of **3-10** with ^{1}H high-power decoupling at 6 kHz.

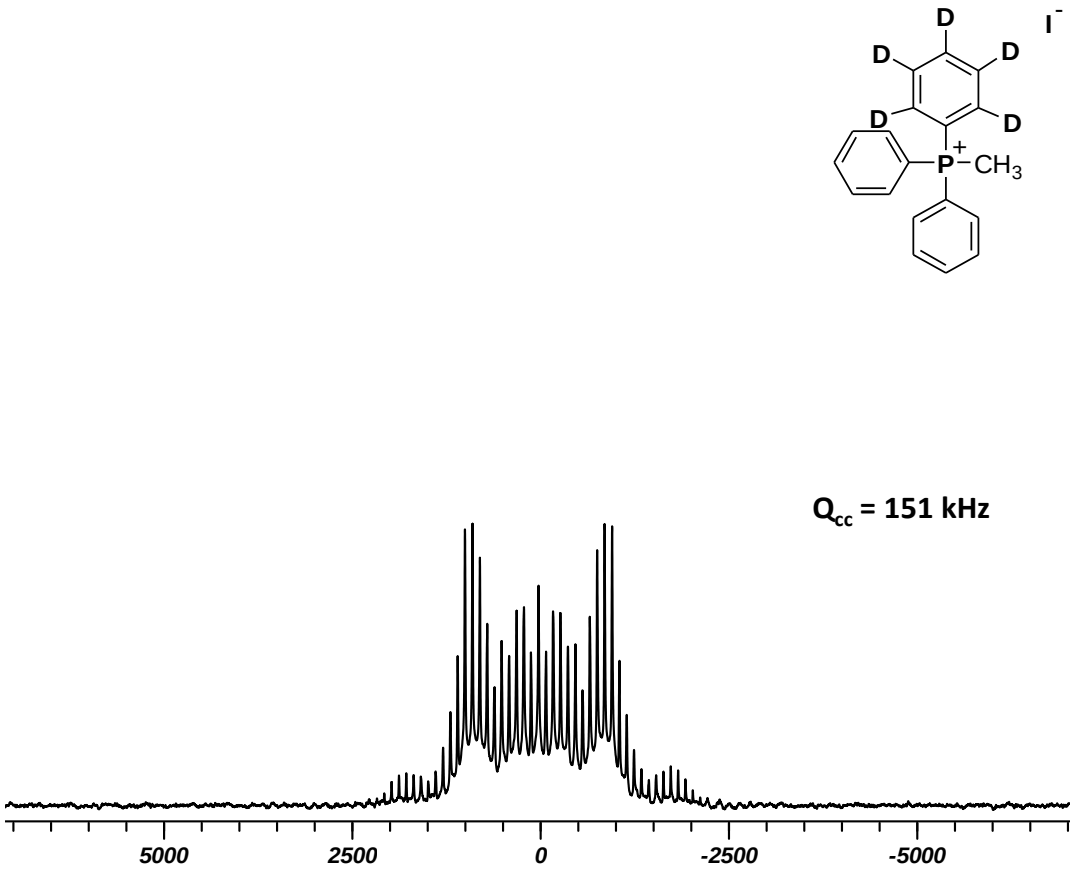

Figure 4-3. ^{2}H MAS NMR of **3-11** with ^{1}H high-power decoupling at 6 kHz.

When **3-10** was adsorbed on the surface, the resulting **3-10a** showed what appeared to be the presence of isotropic motion, along with a wideline pattern at the base which would indicate a static system (Figure 4-4). This phenomenon might be due to the presence of multiple layers as the surface coverage for **3-10a** was 114 particles/100 nm^2, which is more than the calculated monolayer of 30 particles/100 nm^2, however, such a scenario would have been detected in ^{31}P MAS spectrum measured of **3-10a**. The isotropic line represents that the surface-adsorbed deuterated phosphine is mobile

enough that even the quadrupolar interactions are reduced substantially. Our attention then was focused on the adsorption of phosphonium salts (Scheme 4-2).

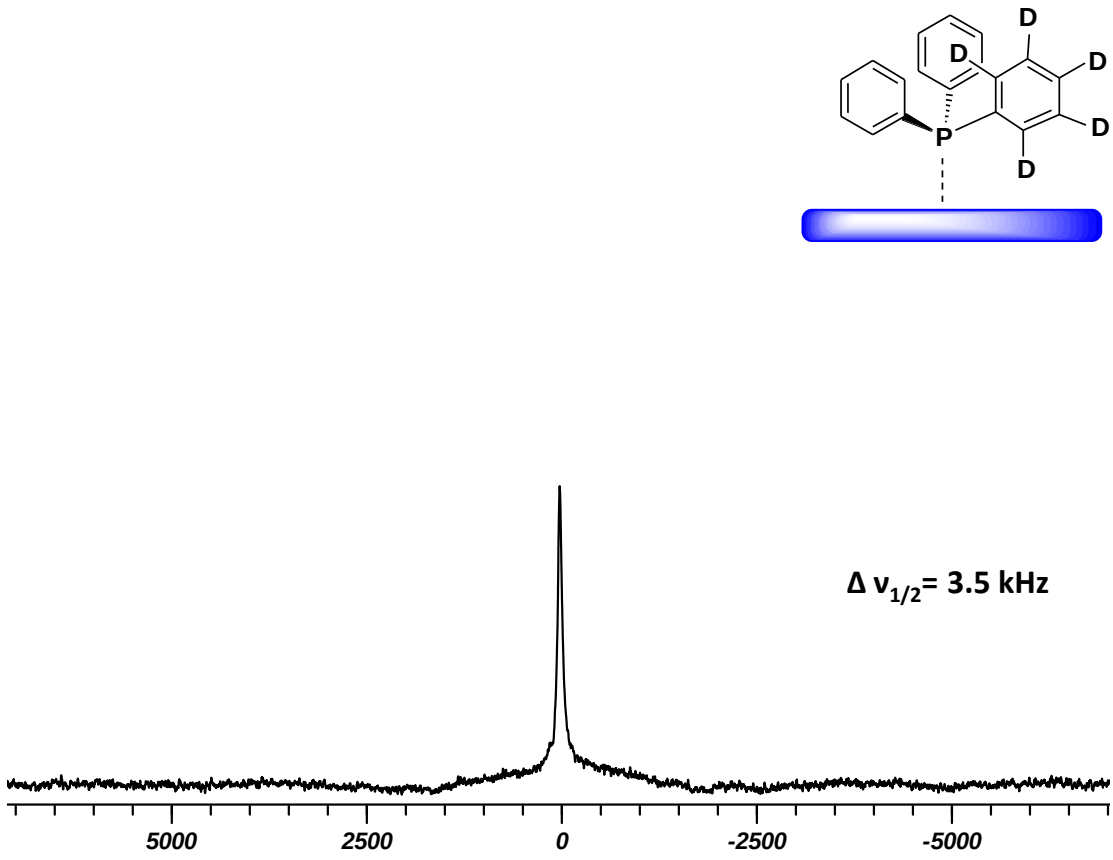

Figure 4-4. ^{2}H MAS NMR of **3-10a** with ^{1}H high-power decoupling at 6 kHz.

Scheme 4-2. Phosphonium salts bound electrostatically to SiO_2 in a monolayer.

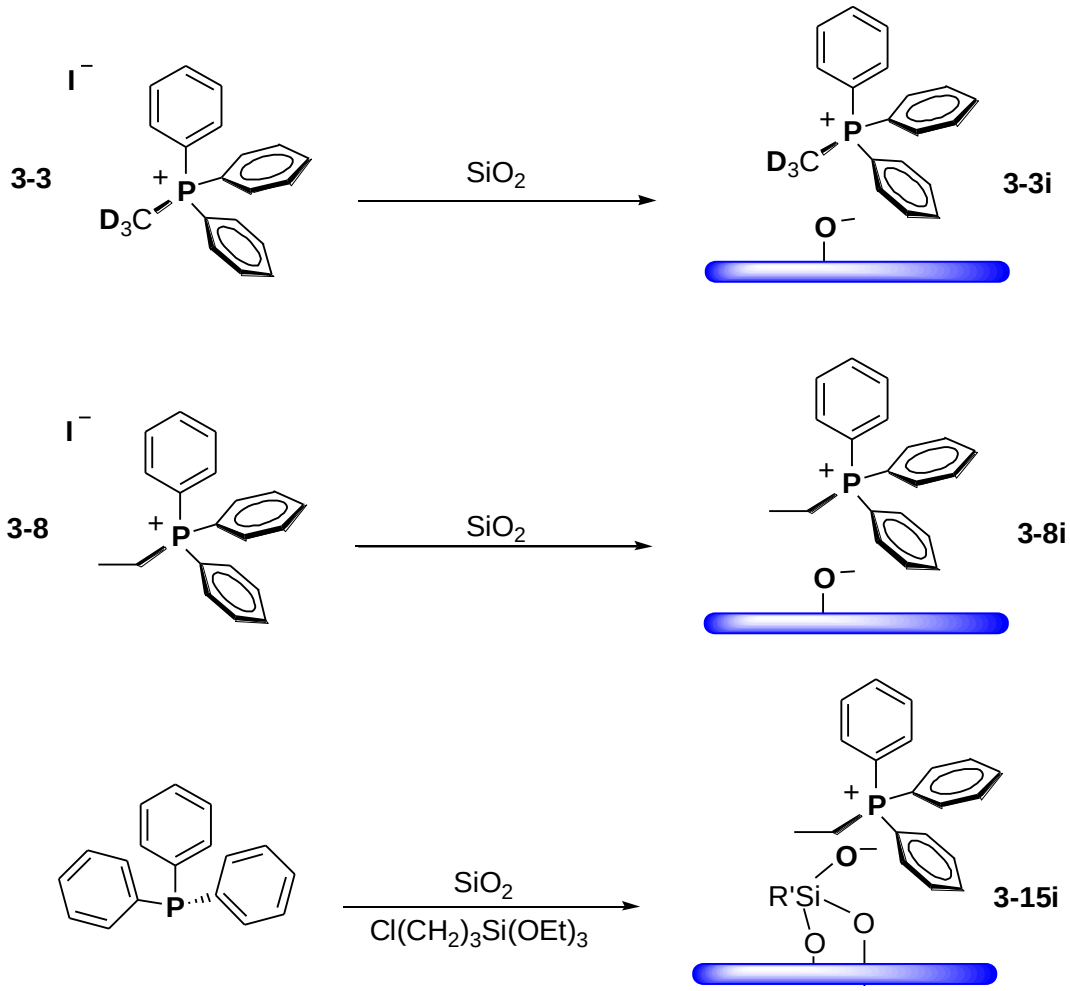

The static measurement of polycrystalline **3-3** displayed a quadrupolar coupling constant (Q_{cc}) of 50.13 kHz (Figure 4-5). From this Q_{cc} of the Pake pattern displayed in Figure 4-5, it is obvious that there is mobility in the molecule. The Q_{cc} value of 50.13 kHz can be attributed to the methyl group rotation about the P-C bond. Similar results

were obtained for **3-3i** that displayed a static Q_{cc} of 52.75 kHz, as expected. For **3-3i** the Q_{cc} is also due to the rapid rotation of the CD_3 group.[25]

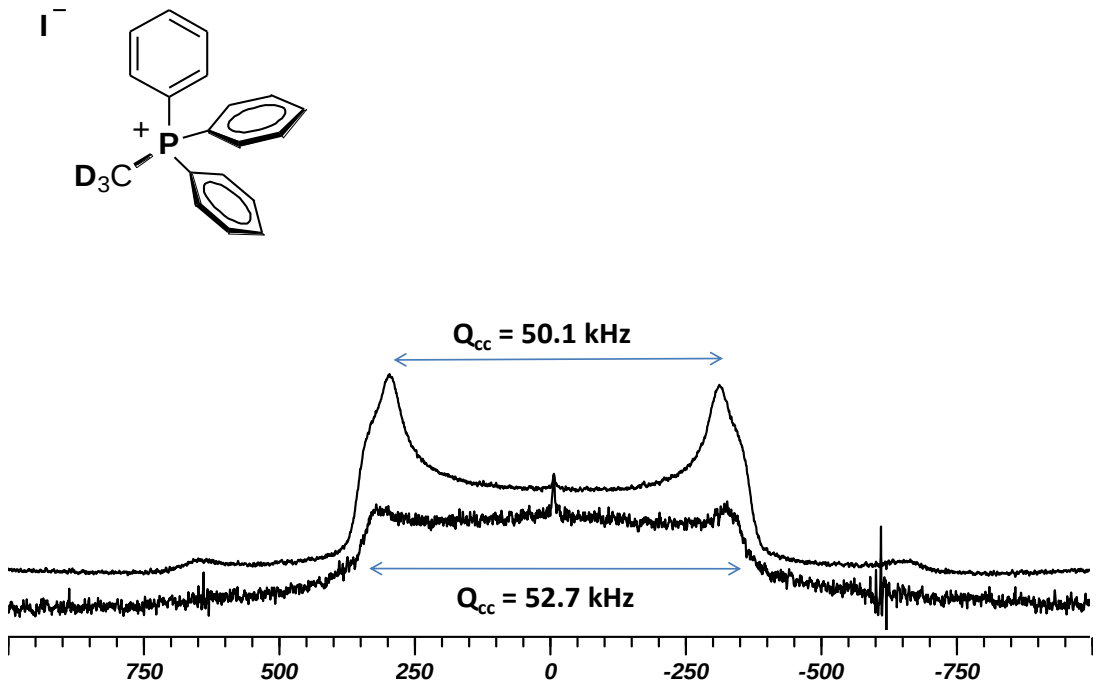

Figure 4-5. ^{2}H Hahn-Echo static spectra of polycrystalline **3-3** (above) and immobilized species **3-3i** (below).

The most promising system, the rigid linker Sn(*p*-$C_6H_4PPh_2)_4$ (**3-12**) was synthesized from the corresponding precursor Sn(*p*-$C_6H_4Br)_4$ and immobilized by forming one, two, or three phosphonium groups that are attached to the silica support by electrostatic interactions (Figure 2-12). In addition, **3-13** and **3-13i** were synthesized and fully characterized, but will be discussed later. The ^{31}P MAS NMR signal of **3-3i** has a $\Delta\nu_{1/2}$ of 574 Hz (Figure 4-6), which indicates substantially more mobility than **3-13i**,

whose $\Delta\nu_{1/2}$ was about 1 kHz (Figure 4-7). Unlike **3-3i**, when measured with ^{31}P HRMAS, **3-13i** gave no ^{31}P NMR signal. This indicates that the interactions between the surface and the phosphonium groups of **3-13i** result in a more strongly and statically immobilized species.

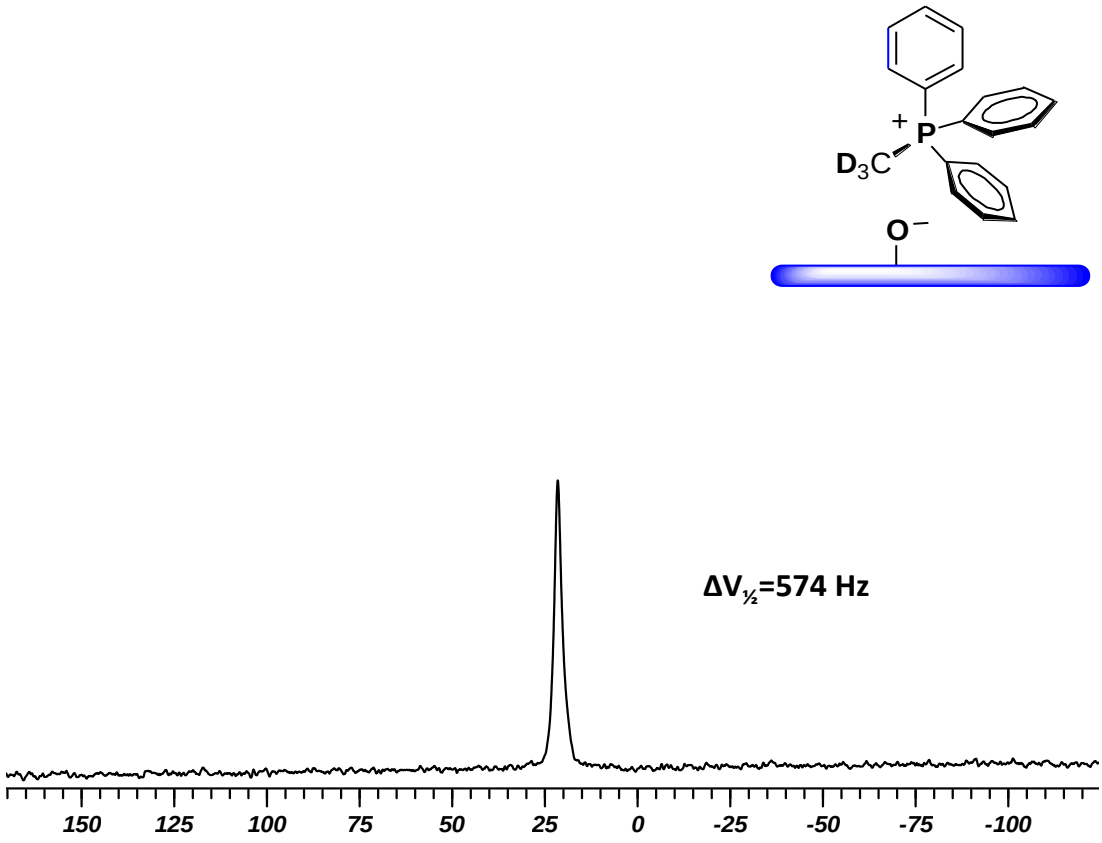

Figure 4-6. ^{31}P MAS NMR of **3-3i** with ^{1}H high-power decoupling.

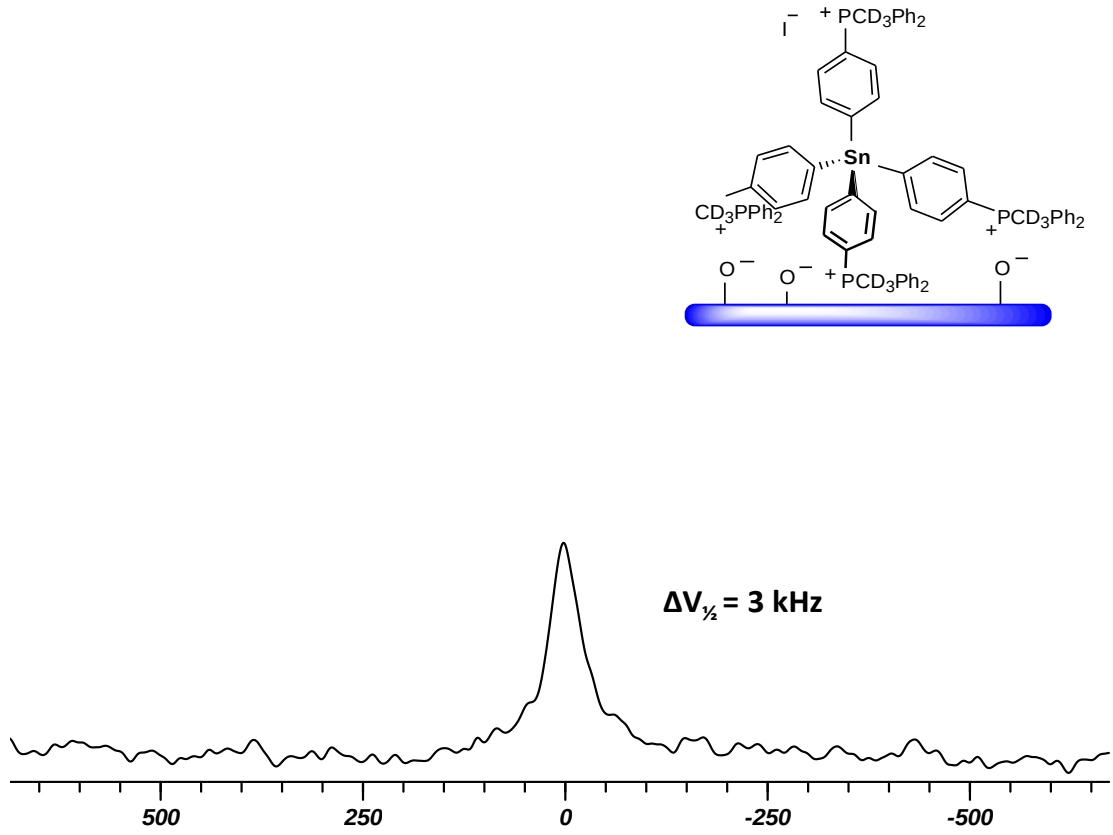

Figure 4-7. ^{2}H HRMAS NMR of **3-13i** with ^{1}H high-power decoupling.

^{2}H HRMAS of **3-3i** displayed an isotropic line (Figure 4-8). On the other hand, **3-16i**, which was synthesized by the methylation of **3-12i** with CD_3I, displayed no peak. Ideally, a Pake pattern would be expected, but its absence could be due to the need of a much longer measurement time and better S/N ratio. This could also indicate that unlike **3-3i**, which might be able to move translationally on the surface, the more rigid system, anchored by three feet, results in a more static linker.

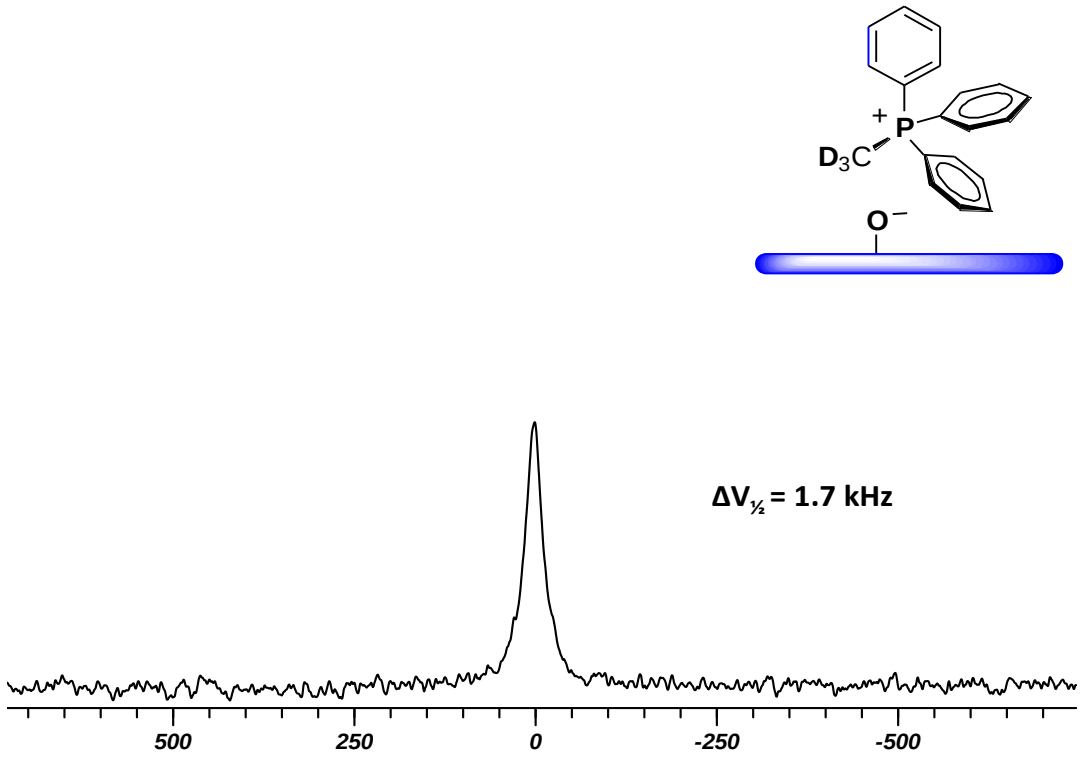

Figure 4-8. ^{2}H HRMAS NMR (Hahn-Echo sequence) of **3-3i** at 2 kHz in toluene.

To better understand the mobility of the phosphonium salts on the surface **3-15i** was synthesized and characterized. The ^{31}P CP/MAS NMR signal of **3-15i** has a $\Delta\nu_{1/2}$ of 632 Hz (Figure 4-9). On the other hand, **3-15i** showed no signal when ^{31}P HRMAS NMR was measured. This result is similar to **3-12i** which also did not show a ^{31}P HRMAS NMR signal and it is a direct indication that the interaction between the surface and the immobilized phosphonium salt formed *in situ* is much stronger than the bonding of the phosphonium salt adsorbed on the SiO_2.

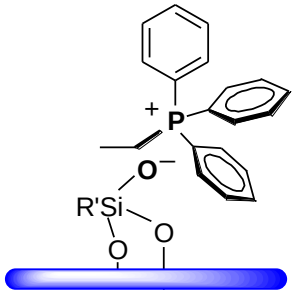

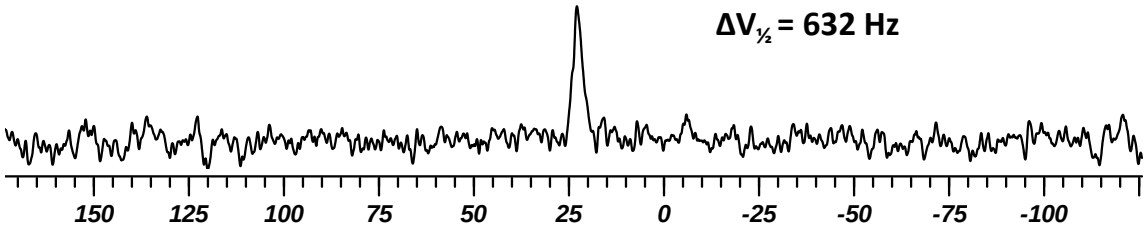

Figure 4-9. ^{31}P CP/MAS NMR signal of **3-15i**.

Surface mobilities of the model phosphonium salt **3-3** on SiO_2 (**3-3i**), both as a monolayer without solvent, and in the presence of solvent, was studied via ^{31}P and ^{2}H CP/MAS and HRMAS. The solvent should have an effect on all modes of mobility, which is why, in analogy to previous studies, special attention was given to the solvent influence. **3-3i** was measured in a series of solvents and their $\Delta\nu_{1/2}$ were determined at 2 kHz and 0 kHz (Table 4-1, Figure 4-10). Earlier studies without sample rotation[61b] have shown that the ^{31}P NMR linewidths obtained from slurries of immobilized linkers are

dependent on the solvent. In general, the less viscous and more polar the solvent is, the narrower the signals are. This is in accordance with the ^{31}P HRMAS signals of the linkers presented in Table 4-1. The resulting ^{31}P HRMAS signal of **3-3i** results in the smallest linewidth of 95 Hz, which is attributed to DMSO, the most polar solvent.

Table 4-1. Halfwidths of the ^{31}P and ^{2}H HRMAS signals of **3-3i** and the ^{31}P HRMAS resonances of **3-13i** at 2 and 0 kHz.

Solvent	^{31}P HRMAS of **3-3i** $\Delta\nu_{1/2}$ at 2 kHz (Hz)	^{31}P HRMAS of **3-3i** $\Delta\nu_{1/2}$ at 0 kHz (Hz)	^{2}H HRMAS of **3-3i** $\Delta\nu_{1/2}$ at 2 kHz (Hz)	^{31}P HRMAS of **3-13i** $\Delta\nu_{1/2}$ at 2 kHz (Hz)	^{31}P HRMAS of **3-13i** $\Delta\nu_{1/2}$ at 0 kHz (Hz)
Toluene	178	450	2.2 kHz	569	1.7 kHz
Et_2O	257	402	3.0 kHz	770	2.3 kHz
DCM	109	260	430	343	660
THF	161	334	1.3 kHz	462	856
Acetone	178	237	430	213	462
MeOH	130	273	379	142	355
MeCN	107	320	413	165	426
DMSO	95	344	356	118	319

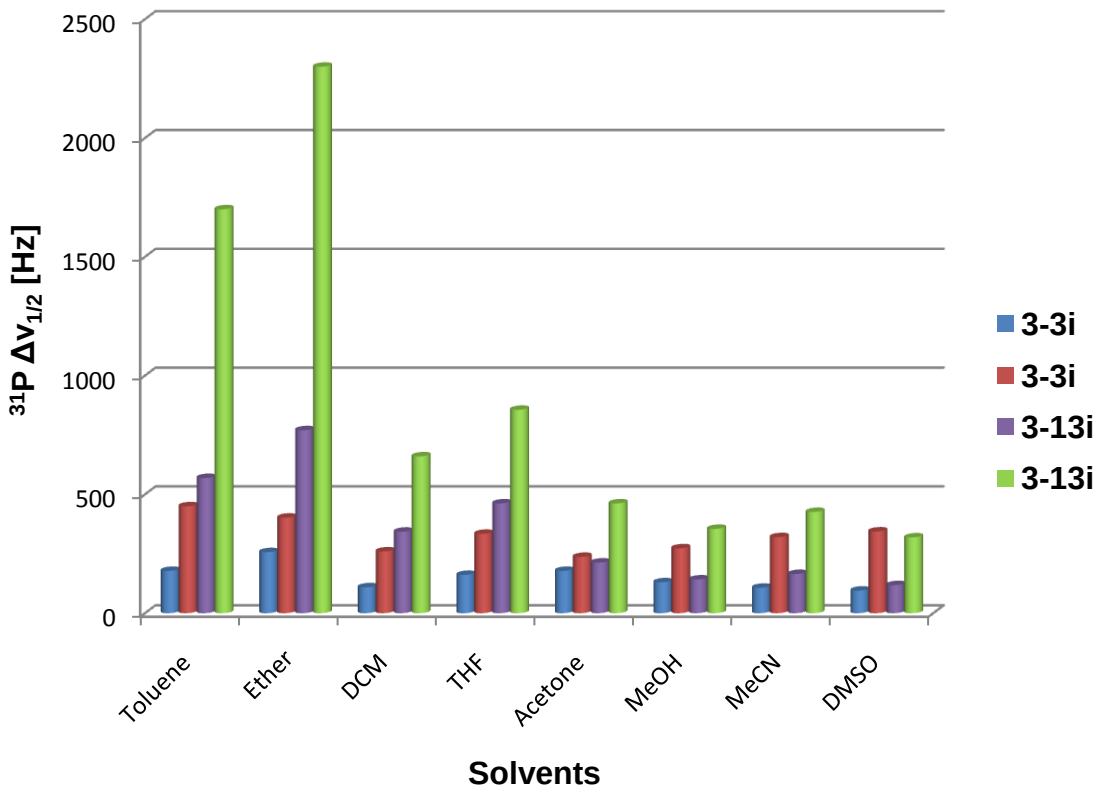

Figure 4-10. Halfwidths of the ^{31}P HRMAS signal of **3-3i** and **3-13i** at 2 and 0 kHz.

Table 4-2 also shows similar trends, with the signal halfwidths of **3-5i**, **3-6i**, **3-7i**, and **3-8i** being largest in DMSO.

Table 4-2. ^{31}P HRMAS halfwidths of several phosphonium salt signals at 2 and 0 kHz.

Solvent	**3-5i** $\Delta\nu_{1/2}$ at 2 kHz (Hz)	**3-5i** $\Delta\nu_{1/2}$ at 0 kHz (Hz)	**3-6i** $\Delta\nu_{1/2}$ at 2 kHz (Hz)	**3-6i** $\Delta\nu_{1/2}$ at 0 kHz (Hz)	**3-7i** $\Delta\nu_{1/2}$ at 2 kHz (Hz)	**3-7i** $\Delta\nu_{1/2}$ at 0 kHz (Hz)	**3-8i** $\Delta\nu_{1/2}$ at 2 kHz (Hz)	**3-8i** $\Delta\nu_{1/2}$ at 0 kHz (Hz)
Acetone	328	231	368	465	172	397	281	479
MeOH	207	456	296	331	284	311	311	438
MeCN	237	402	222	474	346	441	308	453
DMSO	334	491	322	518	325	432	343	450

Furthermore, the linewidths are smaller for the more polar solvents, such as dichloromethane, acetonitrile and methanol, while the less polar and less viscous solvent diethylether leads to a broader line with a halfwidth of 257 Hz. The ^{31}P HRMAS signals of the linkers without spinning lead to less concise results. However, the ^{2}H HRMAS results are in agreement with the trends observed with the ^{31}P HRMAS signals of the

linkers spun at 2 kHz. The resulting phosphine signal of **3-3i** results in the smallest linewidth of 356 Hz in DMSO, the most polar solvent, and the largest linewidth of 3.0 in Et_2O, the least polar of the chosen solvents.

However, in comparison to **3-3i**, for **3-13i** the $\Delta\nu_{1/2}$ are much larger at both 2 and 0 kHz, the broadest signal (770 Hz, 2.3 kHz) being obtained again in Et_2O and the narrowest (118 Hz, 319 Hz) in DMSO. This is no surprise, because **3-13i** is a more rigid scaffold with 3 "feet" anchored to the SiO_2 surface via electrostatic interactions. **3-13i** also has several binding sites per molecule, which might impede the translational mobility on the surface by statistically “pulling in different directions”. However, the scaffold is not as rigid as **3-12i**, which is covalently bound to the support. Based on these results, it can be stated that the binding of the tetraarylphosphonium salts to a silica surface is strong. In addition, when reacted with acid or base, the arylphosphonium salts proved to be impossible to remove form the support in substantial amounts, without dissolving the oxide support. The same result was obtained when anion exchange with NaI and LiCl was performed. Also, when nucleophillic reagents such as NaOEt and KO^tBu was reacted with the surface-bound phosphonium salts, little surface-bound phosphonium was removed.[70]

4.2 Leaching of Linkers

One of the major issues for immobilized catalysts is leaching or detachment of the linker from the support. Therefore, the leaching of the arylphosphonium salt **3-4i** was studied quantitatively. To study the leaching using ^{31}P NMR, a known concentration of the phosphonium salt was integrated with respect to an internal standard. Using the same standard and NMR tube proved to be a convenient and reliable method for monitoring the phosphonium leaching quantitatively. The leaching tests reveal that no leaching occurs in the least polar solvents toluene, Et_2O, and DCM. Furthermore, it is to be noted that with toluene, the solvent of choice for catalysis, no measurable detachment of the phosphonium salt was observed. However, more polar solvents, such as DMSO and MeCN, do lead to substantial leaching (Figure 4-11). The leaching result was based on the integration of the standard signal and that of the phosphonium salt, whose δ was 23.0 ppm. In order to check, whether the calibration was correct, the leaching was also determined gravimetrically. Both tests gave the same results within the error margins.

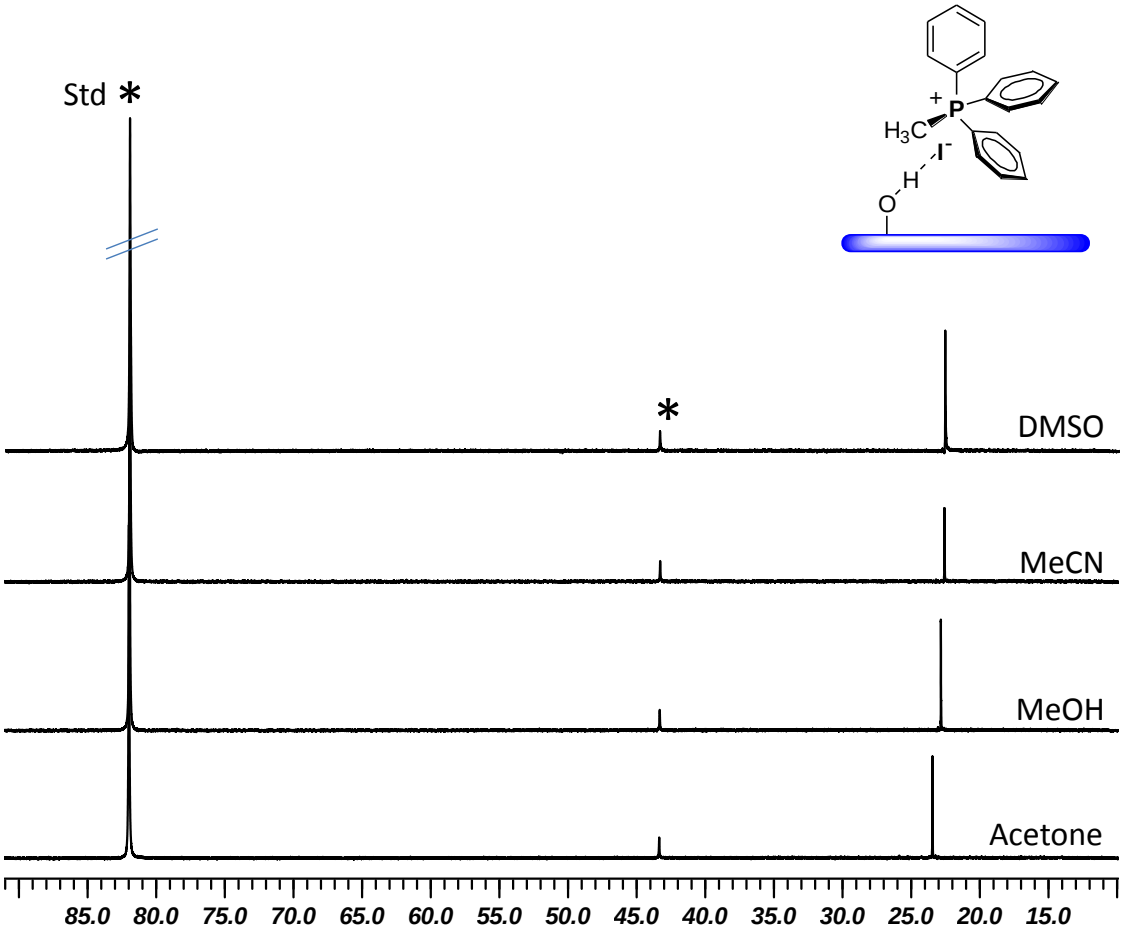

Figure 4-11. ^{31}P NMR of **3-4i** leaching in more polar solvents. The asterisks denote the signals of the standard $ClPPh_2$ in the capillary (81.9 ppm), and traces of its oxide at 43.0 ppm.

As an additional parameter to be considered, the solubility of the phosphonium salts in the given solvents do play a role, as seen in the increase in leaching of **3-4i** in MeOH (Figure 4-12).

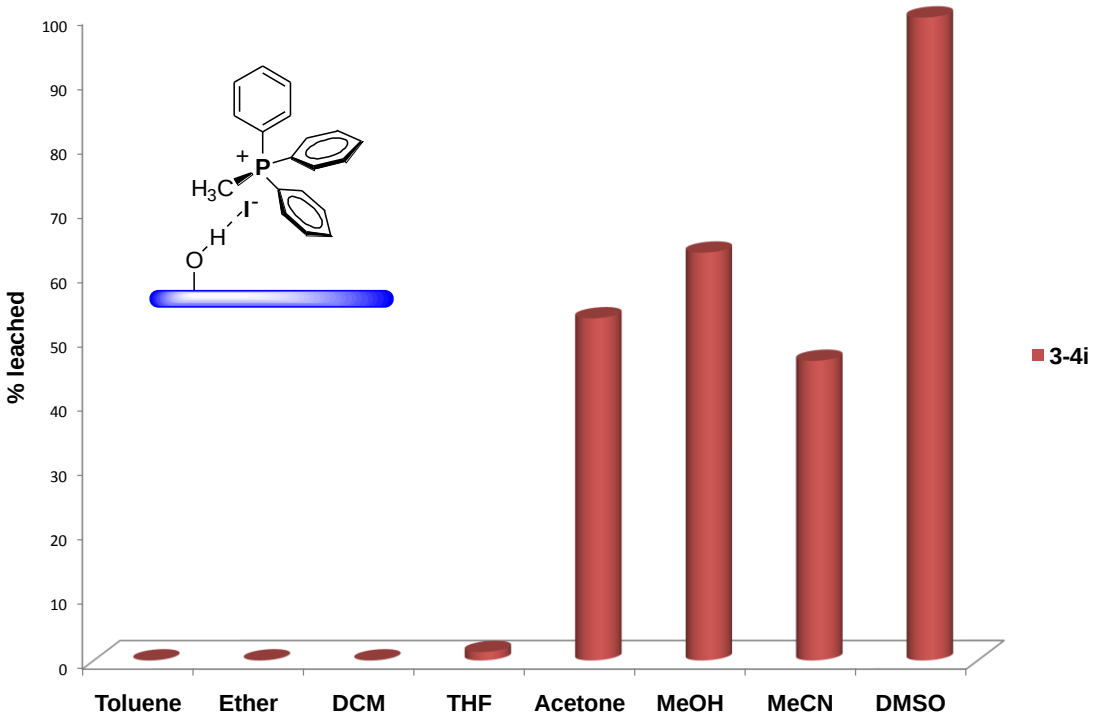

Figure 4-12. Graphic display of the leaching studies for the model phosphonium salt **3-4i**.

4.3 Influence of the Counteranion on Binding

Although the mobilities of the linkers and the catalysts are crucial factors for the performance and design of the immobilized catalyst, the mode of binding is unknown and often discussed in the literature, for example, as hydrogen bonding between the F atoms in BF_4^- and surface silanol protons.[71] For these reasons, the influence of the counteranion on the binding of the phosphonium salts on silica is of utmost interest. The phosphonium salts depicted in Figure 4-13 were immobilized on SiO_2 and their detachment was studied in the most favorable solvents for "medium amount" leaching, based on preliminary results (Figure 4-11).

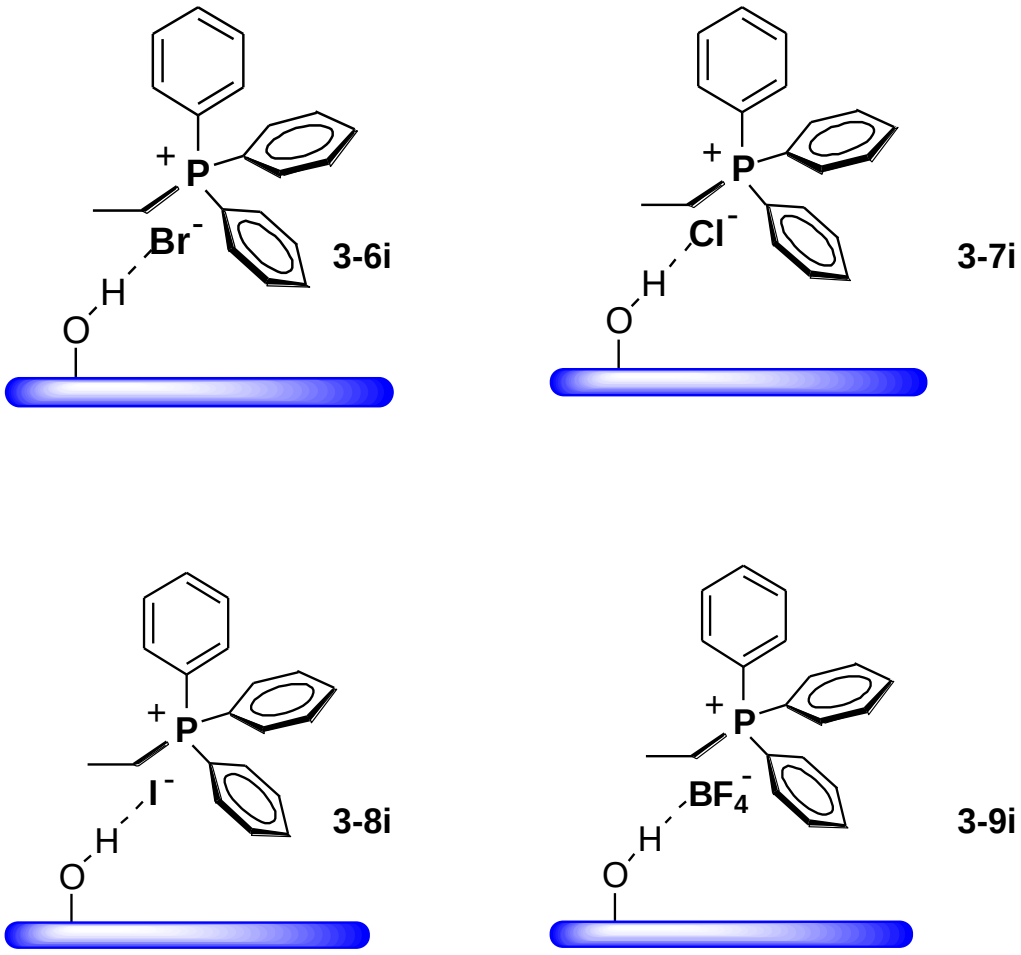

Figure 4-13. Phosphonium salts used to probe the influence of the counteranion.

The results from Figure 4-14 show that the counteranion does have an influence. This is particularly observed in MeCN, a solvent that the surface-bound phosphonium salt **3-4i** leached moderately in.

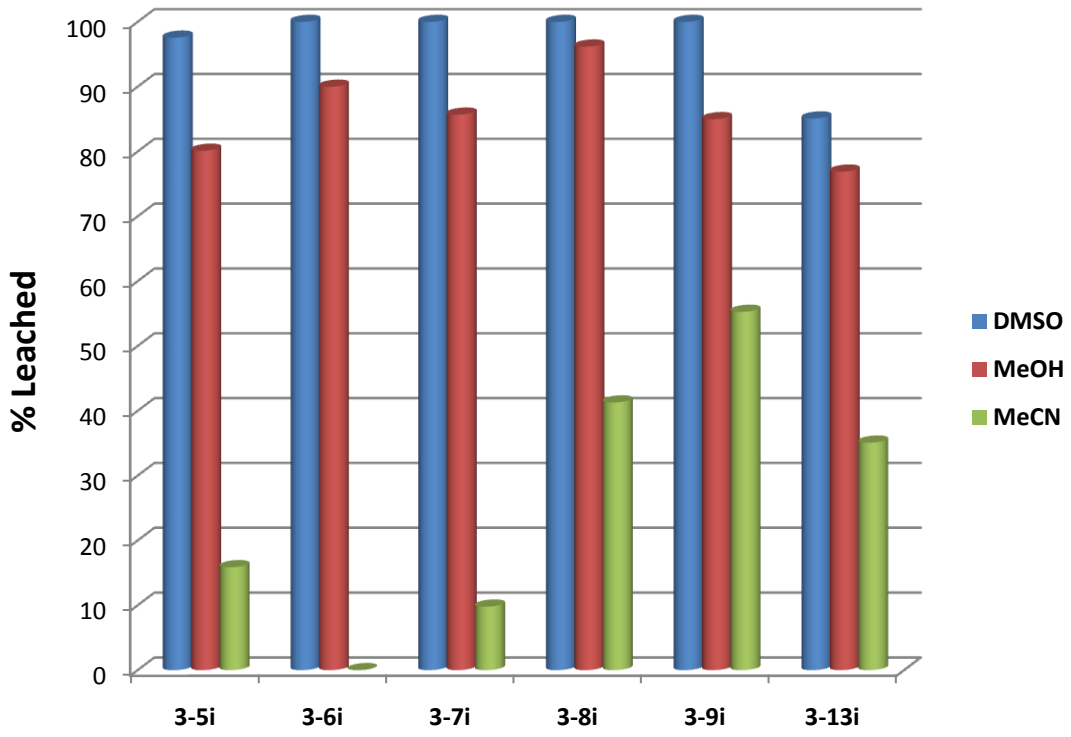

Figure 4-14. Leaching of immobilized phosphonium salts.

The leaching studies reveal that all phosphonium salts are detached from the surface by the more polar solvents, such as DMSO and MeOH. The influence of the counteranion on leaching is observed best in MeCN, the solvent that had led to moderate leaching. These results show that the leaching of the phosphonium salts follow this order: BF_4^- > I^- > Br^- > Cl^-. Another interesting result showed that **3-13i**, which is the more rigid tetraphosphonium scaffold, leaches less than all the other phosphonium salts (**3-5i**, **3-6i**, **3-7i**, **3-8i**, and **3-9i**), which can be caused by the different solubility, as well

as by the attachment of **3-13i** via ‘3 feet’ to the SiO_2 surface, instead of only one. Therefore, the detachment of **3-13i** from the surface requires the concerted removal of 3 "feet", and this is statistically less likely than the detachment of just one phosphonium group.

4.4 Tetraphosphonium Salt Characteristics

Besides the chemical shift and the linewidth, solid-state NMR provides another useful parameter for investigating surface-bound systems, the CSA, along with its principal components δ_{11}, δ_{22}, and δ_{33}. The bottom spectrum of Figure 4-15 shows a rather narrow CSA for the signal of **3-13i**. Using the simulation software program WSolids[72] the CSA of **3-13i** was determined to be 18 ppm and had a δ_{11} of 28 ppm, a δ_{22} of 19 ppm, and a δ_{33} of 10 ppm. These results correspond well to previous CSA values of alkyl phosphonium salts, whose wideline signals are also narrow, between 20 to 44 ppm in width.[73] The reduction of the CSA of **3-13i** could be due to the ability of the phosphonium salt to move over the surface, since there is no directional covalent interaction, but rather an electrostatic interaction with the surface.

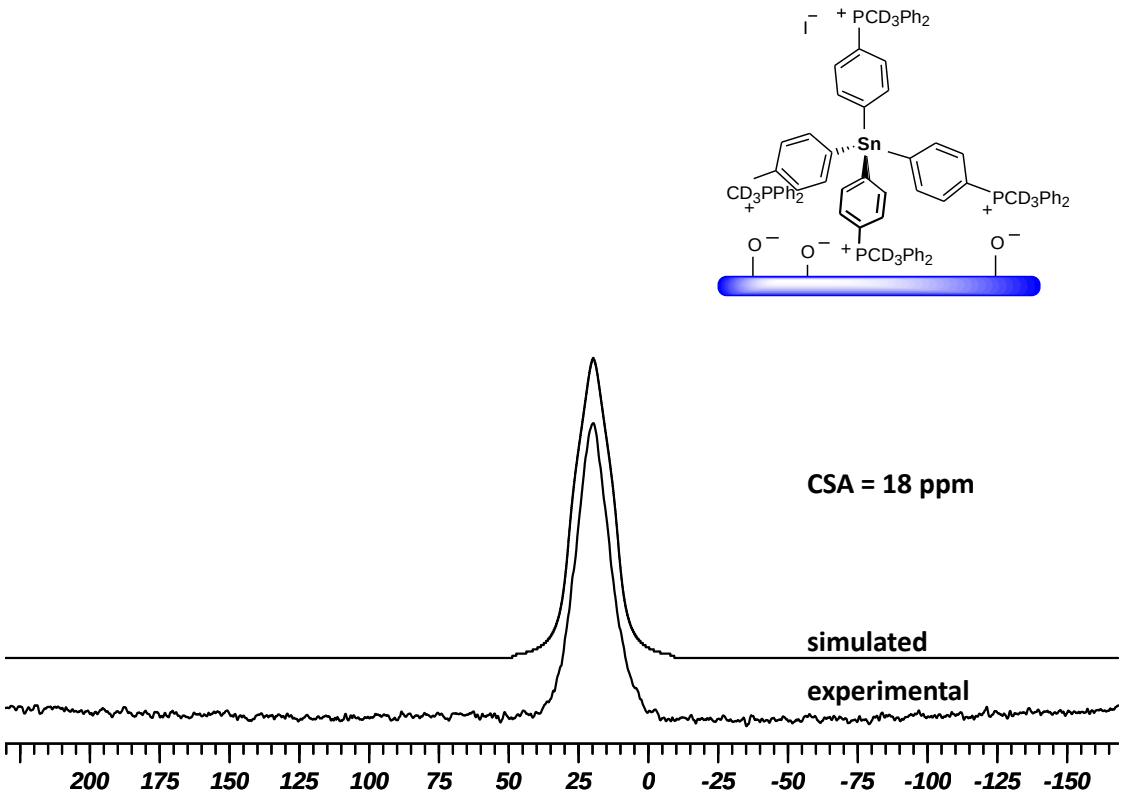

Figure 4-15. ^{31}P CP/MAS wideline spectrum (0 kHz) of **3-13i** (bottom) and simulated spectrum (top).[72]

A noteworthy feature of the molecular compound **3-13** in solution is, that the ^{119}Sn NMR spectrum showed an interesting long-range $^{5}J(^{119}\text{Sn-}^{31}\text{P})$ coupling of 19.7 Hz (Figure 4-16).

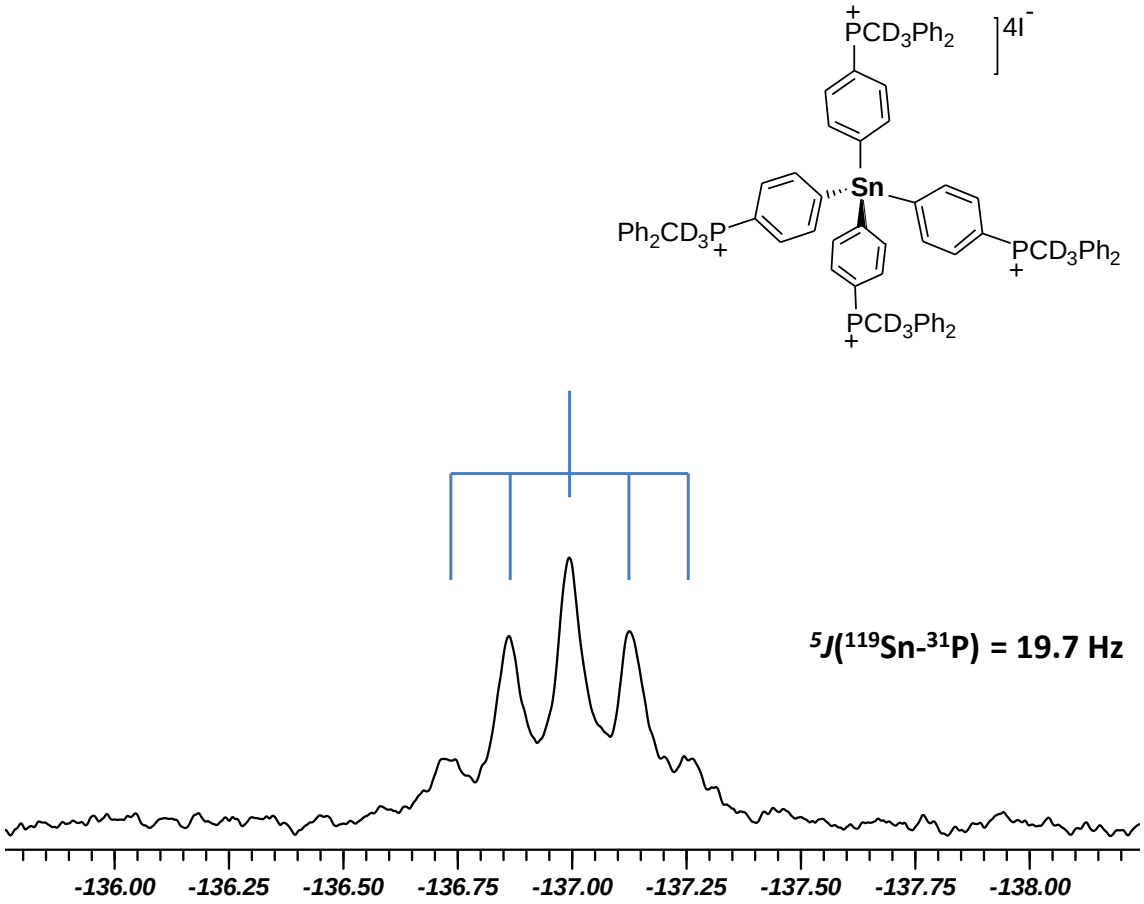

Figure 4-16. ^{119}Sn NMR spectrum (CD_2Cl_2) of **3-13**.

Coupling between ^{119}Sn and other nuclei over four or more bonds is not unexpected in molecules with a rigid framework, but it is not often observed. Interestingly, the tetraphosphine version of the molecule, **3-12**, does not show this coupling.[6] However, the data is limited with respect to diagnostic conclusions regarding the propagation of the coupling through the bonds.[74] To reinforce our findings, additionally compound **3-14** was synthesized and it displayed a $^{5}J(^{119}\text{Sn}\text{-}^{31}\text{P})$ coupling with 18.9 Hz (Figure 4-17), and therewith a value in the same range.

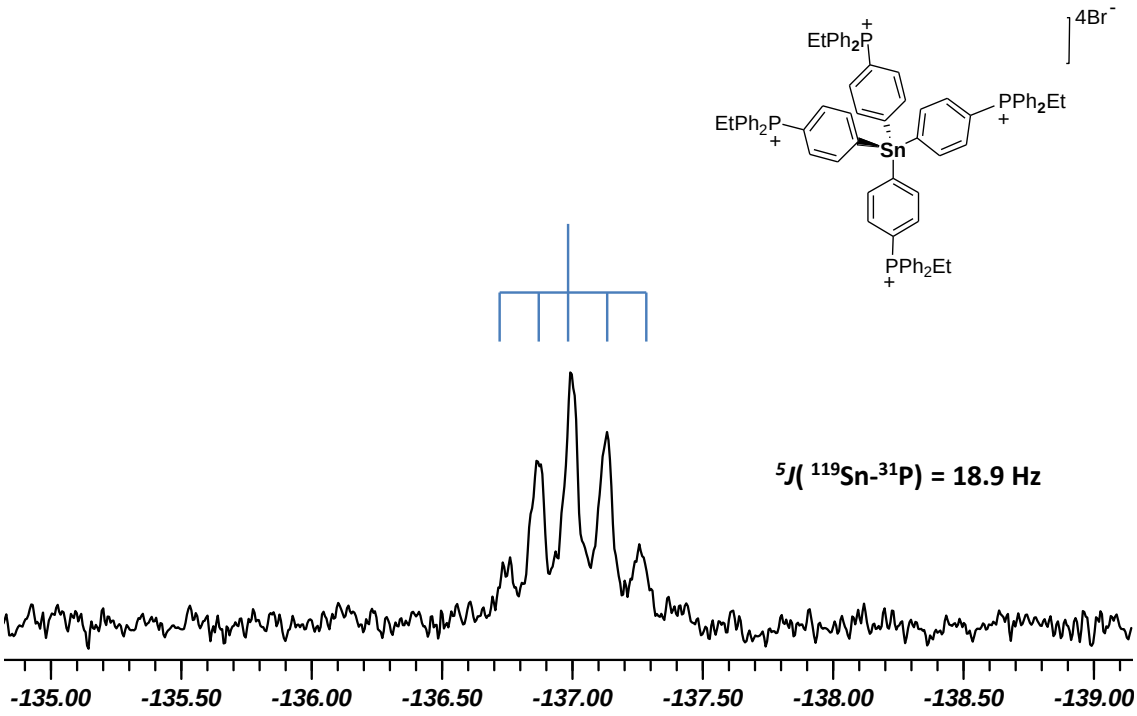

Figure 4-17. ^{119}Sn NMR spectrum (CD_2Cl_2) of the tetraphosphonium bromide **3-14**.

4.5 Catalysis

A key step in the synthesis of the immobilized catalysts is the tethering of the linkers to the silica surface, as shown in Scheme 4-3. In this project, the immobilization via three phosphonium groups was sought. Therefore, a solution of the linker **3-12** in toluene and a 100-fold excess of (3-chloropropyl)triethoxysilane was added to a suspension of silica in toluene. The suspension was stirred for seven days at 90°C to obtain the 3-fold binding to the surface.

Scheme 4-3. Immobilization of the tetraphosphines on the silica surface.

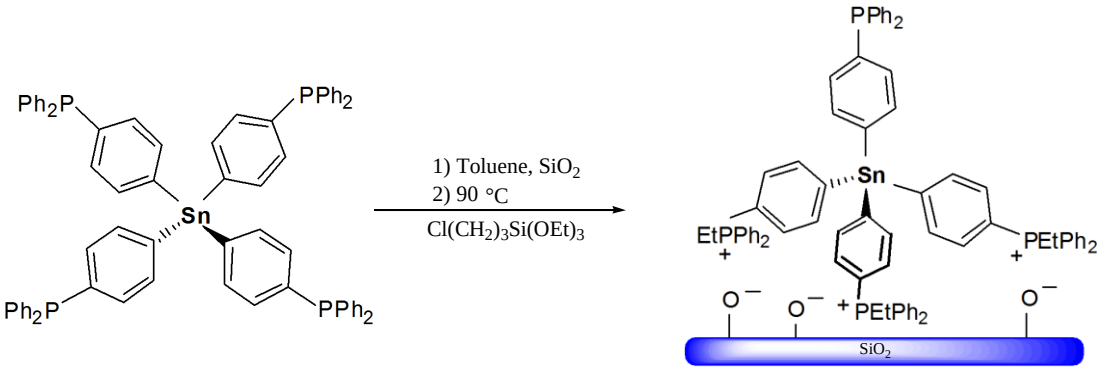

(3-Chloropropyl)triethoxysilane is used to functionalize the silica, because it is inexpensive and readily available. The reason for the 100-fold excess is, that a binding via three phosphonium moieties is only obtained with this large excess, together with a prolonged reaction time. Former studies in the Bluemel group showed that, with silica prefunctionalized by a submonolayer amount of ethoxysilane, only one phosphonium

moiety is bound. A 10-fold excess of the silane leads to two surface-bound phosphonium groups.[16]

In order to determine whether the linker was bound to the surface via three phosphonium groups, leaving one phosphine group unchanged, quantitative ^{31}P MAS spectra were recorded. In Figure 4-18 the ^{31}P MAS NMR of the immobilized tetraphosphine **3-12i** is shown.

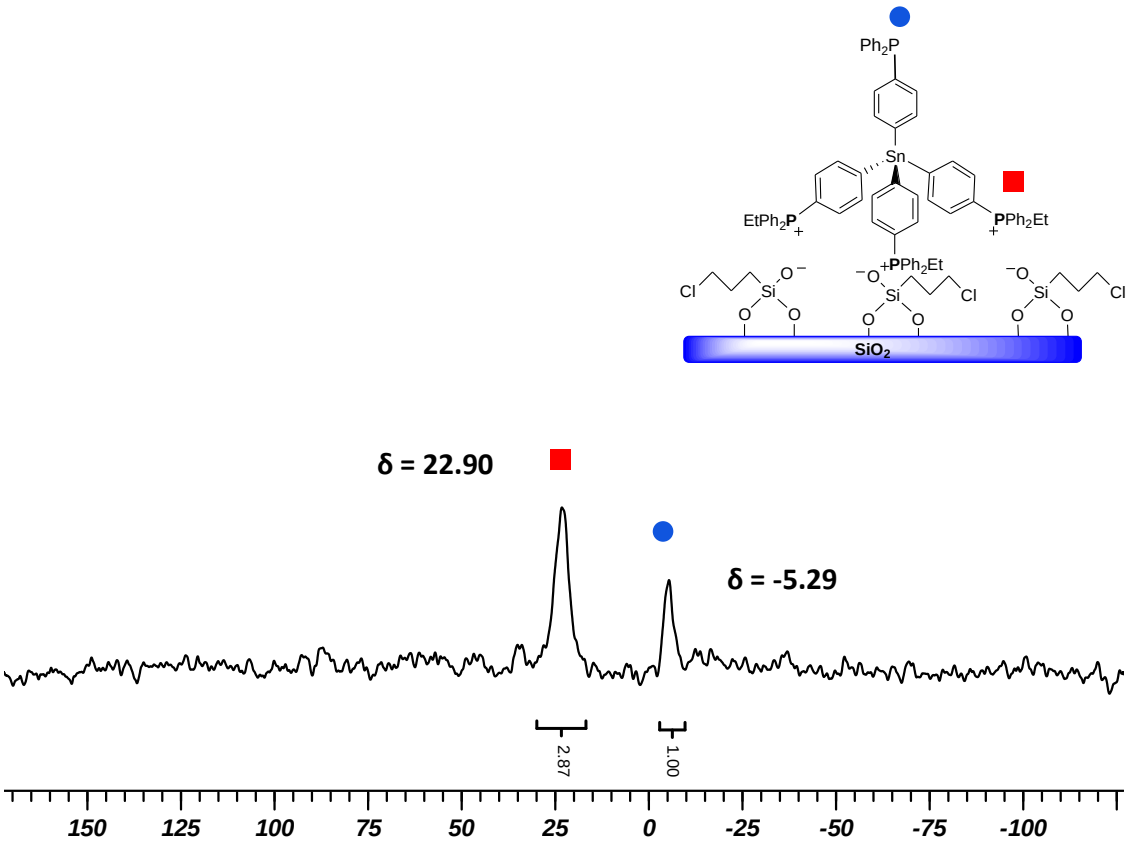

Figure 4-18. ^{31}P MAS NMR spectrum of immobilized **3-12i**; ν_{rot} = 9 kHz.

The chemical shift of the phosphonium group (δ = 22.9 ppm) was in good agreement with the literature (δ = 24 ppm).[16] The chemical shift of the non-quaternized phosphine is δ = -5.29 ppm, and therefore in the range of triphenylphosphine. To make sure that the integrals give the correct intensities of the signals, the pulse delay time was changed. If the delay time is too short, the nuclei cannot relax completely, and hence some integrals appear to be too small. With the change of the delay time from 5 s to 10 s and 20 s, the integrals did not change. Thus, a delay time of 5 s is long enough for all nuclei to relax completely.

Next, the linker was coordinated to a metal complex for applications in catalysis. In order to coordinate a metal to the free phosphine, Wilkinson's catalyst was used. During the immobilization by ligand exchange, PPh_3 was released and therefore the supernatant was decanted, and the silica was washed to remove all liberated triphenylphosphine. In Figure 4-19, the ^{31}P MAS spectra of the immobilized species **3-12i** and **3-17i** are shown. After addition of the metal complex, the phosphonium signal did not change. The free phosphine signal at -5.29 ppm disappears and a new signal at 35.0 ppm appears. The latter signal represents the two PPh_3 groups *cis* to Cl. The signal of the phosphine group *trans* to Cl is not visible in the spectrum, most probably due to the low S/N ratio.

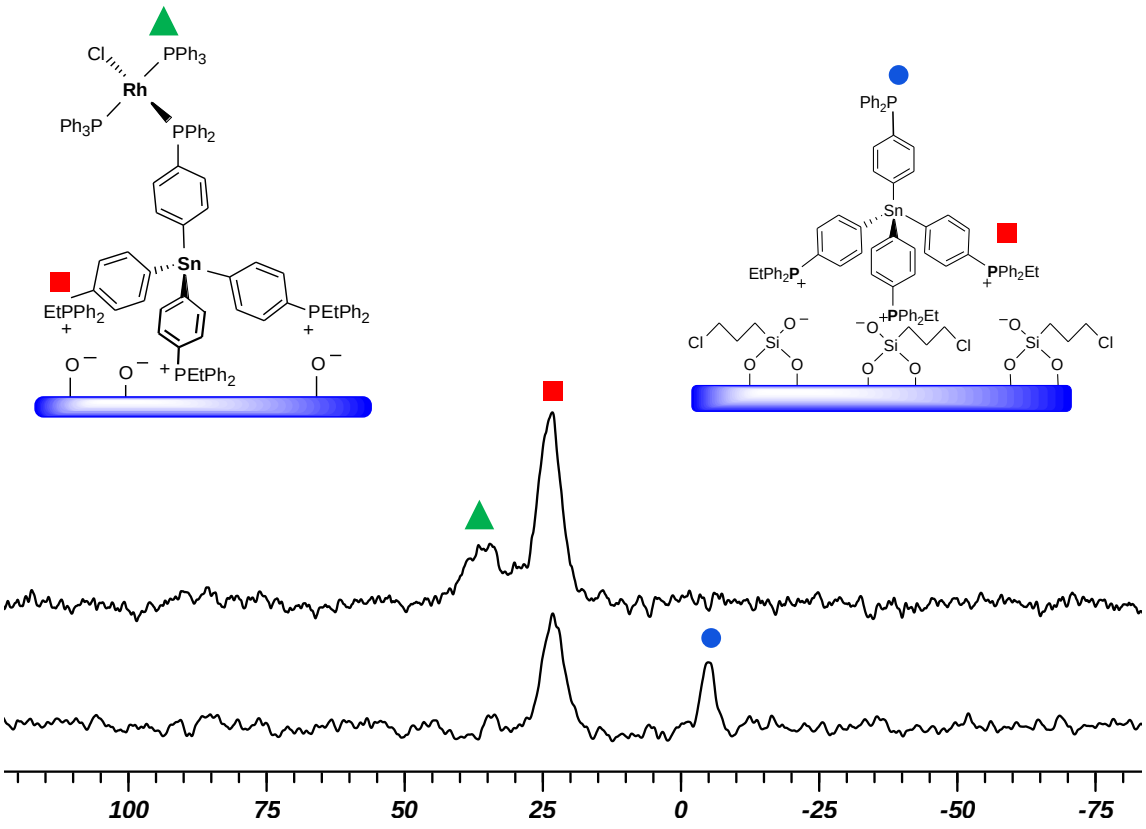

Figure 4-19. ^{31}P MAS NMR spectra of immobilized **3-17i** (bottom) and **3-12i** (top).

Furthermore, a preliminary mobility study of the immobilized rhodium complex **3-17i** was undertaken. For this purpose, a ^{31}P HRMAS NMR spectrum in toluene was recorded, but even after 848 scans, no signal was visible. This means that the immobilized catalyst does not have any translational mobility on the surface and no parts of it are "wiggling" in the presence of the solvent.[75] This finding proves that the tetraphosphine linker scaffolds are truly rigid and stationary, a fact that should lead to superior immobilized catalysts.

Finally, **3-17i** was used to catalyze the hydrogenation of dodecene as described in previous results.[6] However, unlike a previous batch of **3-17i** that was capable of being recycled 30 times within a 24 hour time span,[6] **3-17i** could only reach 50 % conversion in 60 h (Figure 4-20).

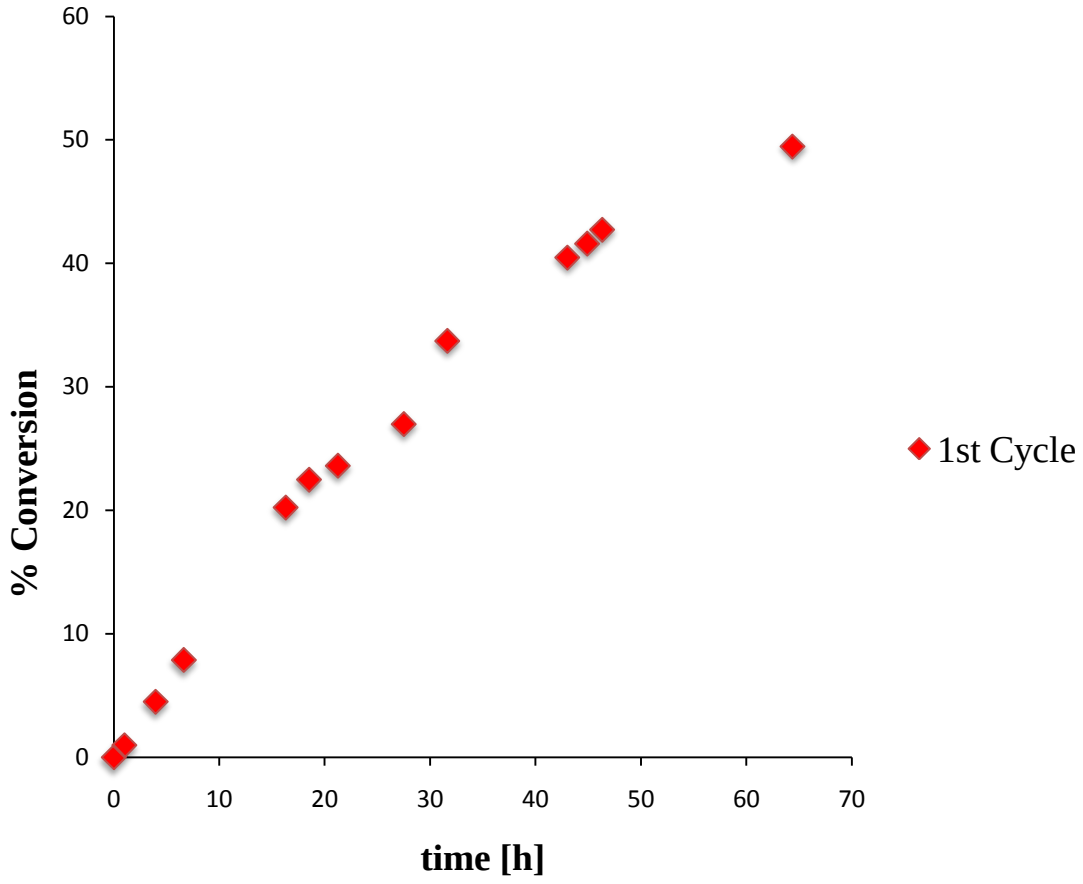

Figure 4-20. Catalysis curve of the hydrogenation of dodecene using **3-17i**.

However, the ^{31}P CP/MAS spectra of the catalyst before and after catalysis were measured (Figure 4-21) and revealed that the phosphonium scaffold bound to the SiO_2 surface remained intact, but the low-field phosphine signal increased in height. This could be due to an oxidation product, explaining the diminished catalytic activity.

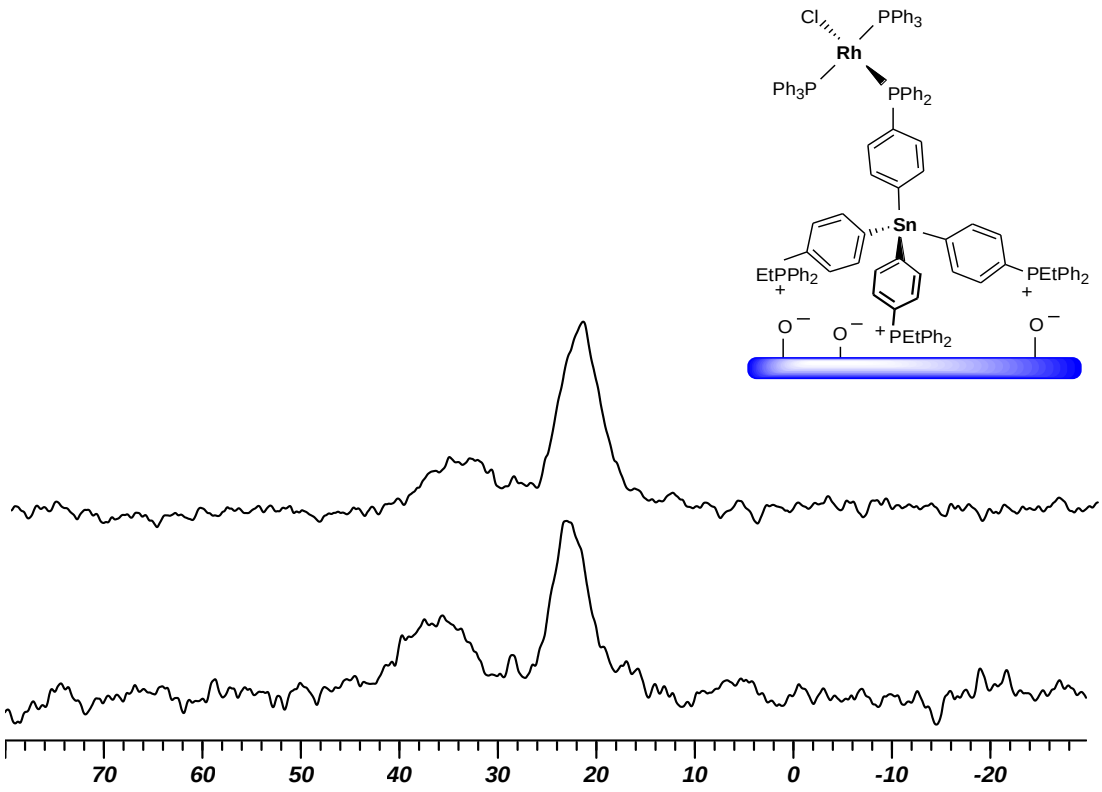

Figure 4-21. ^{31}P CP/MAS of **4-17i** before (top) and after catalysis (bottom).

5. CONCLUSION

The novel rigid tetraphosphine linkers were synthesized and immobilized via the formation of phosphonium groups and by direct reaction of tetraphosphonium salts with oxide surfaces. These studies have shown that unlike previous alkyl linkers that are capable of "bending down", the tetraphosphine linkers immobilized via *in situ* formation of the phosphonium groups on the SiO_2 are very rigid and thus prevent any contact of the metal complex with the reactive silica surface.[6]

In addition, the studies have also shown that phosphines immobilized on oxide supports by adding $Cl(CH_2)_3Si(OEt)_3$ to the reaction mixture lead to phosphonium salts bound to the surface irreversibly. Furthermore, leaching and mobility studies prove that the solvents do play a crucial role, and the more polar solvents (DMSO) exhibit the most extensive leaching due to the solvents' strong adsorption on the SiO_2 surface. Leaching studies also showed that the counteranion does have an influence on the binding of the phosphoniumn salts on the SiO_2 surface. The leaching decreased as follows: $BF_4^- > I^- > Br^- > Cl^-$. This speaks against hydrogen bonding between F and surface-H atoms, but there being an interaction of some sort between the anion and the surface. Future studies on this subject will be continued in the group.

REFERENCES

(1) (a) Nicolaou, K. C.; Hanko, R.; Hartwig, W. Eds. *Handbook of Combinatorial Chemistry*; Wiley-VCH: Weinheim, Germany, 2002; p 1145. (b) Bannworth, W.; Felder, E. Eds. *Combinatorial Chemistry*; Wiley-VCH: Weinheim, Germany, 2000; p 47-95.

(2) (a) Seneci, P. *Solid-Phase Synthesis and Combinatorial Technologies*; John Wiley & Sons: New York, 2000. (b) Dörwald, Z. F. *Organic Synthesis on Solid Phase*; Wiley-VCH: Weinheim, Germany, 2000.

(3) (a) VanDer Voort, P.; Vrancken, K. C.; Vansant, E. F. *Characterization and Chemical Modification of the Silica Surface*; Elsevier: Amsterdam, 1995. (b) Scott, R. P. W. *Silica Gel and Bonded Phases*; John Wiley and Sons: New York, 1993. (c) Subramanian, G. A. *Practical Approach to Chiral Separations by Liquid Chromatography*; VCH: Weinheim, Germany, 1994. (d) Iler, R. K. *The Chemistry of Silica*; John Wiley: New York, 1979.

(4) (a) Hartley, F. R. *Supported Metal Complexes*; D. Reidel Publishing Co.: Dordrecht, The Netherlands, 1985. (b) Clark, J. H. *Supported Reagents in Organic Reactions*; VCH: Weinheim, Germany, 1994. (c) Gladysz, J. A.; The Experimental Assay of Catalyst Recovery: General Concepts. In *Recoverable and Recyclable Catalysts*; 1st Ed. Benaglia, M., Ed. Wiley & Sons: United Kingdom, 2009; Vol. 102, pp 1-14. (d) DeVos, D. E.; Vankelecom, I. F. J.; Jacobs, P. A. *Chiral Catalyst Immobilization and Recycling*; Wiley-VCH: Weinheim, Germany, 2000. (e) Rothenberg, G. *Catalysis: Concepts and Green Applications*; Wiley-VCH: Weinheim, Germany, 2008.

(5) Blümel, J. *Coord. Chem. Rev*. **2008**, *252*, 2410-2423.

(6) Beele, B.; Guenther, J.; Perera, M.; Stach, M.; Oeser, T.; Blümel, J. *New J. Chem*. **2010**, *34*, 2729-2731.

(7) Sibilia, J. P. *A Guide to Materials Characterization and Chemical Analysis*; Wiley-VCH: New York, 1988.

(8) Fyfe, C. A. *Solid-State NMR for Chemists*; C.F.C.: Guelph, Cananda, 1983, and refs. cited.

(9) Engelhardt, G.; Michel, D. *High-Resolution Solid-State NMR of Silicates and Zeolites*; John Wiley & Sons: New York, 1987.

(10) Bell, A. T.; Pines, A. *NMR Techniques in Catalysis*; Marcel Dekker: New York, 1994.

(11) Stejskal, E. O.; Memory, J. D. *High Resolution NMR in the Solid State*; Oxford University: New York, 1994.

(12) Merckle, C.; Blümel, J. *Chem. Mater*. **2001**, *13*, 3617-3623.

(13) (a) Tsiavaliaris, G.; Haubrich, S.; Merckle, C.; Blümel, J. *Synlett* **2001**, 391-393. (b) Piestert, F.; Fetouaki, R.; Bogza, M.; Oeser, T.; Blümel, J. *Chem. Commun*. **2005**, 1481-1483.

(14) (a) Reinhard, S.; Soba, P.; Rominger, F.; Blümel, J. *Adv. Synth. Catal*. **2003**, *345*, 589-602. (b) Reinhard, S.; Behringer, K. D.; Blümel, J. *New J. Chem*. **2003**, *27*, 776-778.

(15) (a) Merckle, C.; Blümel, J. *Topics in Catal*. **2005**, *34*, 5-15. (b) Merckle, C.; Blümel, J. *Adv. Synth. Catal*. **2003**, *345*, 584-588. (c) Merckle, C.; Haubrich, S.; Blümel, J. *J. Organomet. Chem.* **2001**, *627*, 44-54.

(16) Yang, Y.; Beele, B.; Blümel, J. *J. Am. Chem. Soc.* **2008**, *130*, 3771-3773.

(17) Niemantsverdriet, J. W. *Spectroscopy in Catalysis*; VCH: Weinheim, Germany, 1995. (b) Sibilia, J. P. *A Guide to Materials Characterization and Chemical Analysis*; VCH: Weinheim, Germany, 1988.

(18) (a) Stanger, K. J.; Wiench, J. W.; Prusik, M.; Espenson, J. H.; Kraus, G. A.; Angelici, R. J. *J. Mol. Catal*. **2006**, *243*, 158-169. (b) Lucas, N. T.; Hook, J. M.; McDonagh, A. M.; Colbran, S. B. *Eur. J. Inorg. Chem*. **2005**, *3*, 496-503. (c) Mehendale, N. C.; Bezemer, C.; Van Walree, C. A.; Klein Gebbink, R. J. M.; Van Koten, G. *J. Mol. Catal. A* **2006**, *257*, 167-175. (d) Zeidan, R. K.; Dufaud, V.; Davis, M. E. *J. Catal*. **2006**, *239*, 299-306. (e) Nunes, C. D.; Pillinger, M.; Valente, A. A.; Rocha, J.; Lopes, A. D.; Goncalves, I. S. *Eur. J. Inorg. Chem*. **2003**, *21*, 3870-3877. (f) DeClercq, B.; Lefebvre, F.; Verpoort, F. *Appl. Catal. A* **2003**, *247*, 345-364. (g) Heckel, A.; Seebach, D. *Chem. Eur. J*. **2002**, *8*, 559-572. (h) Uusitalo, A.-M.; Pakkanen, T. T.; Iiskola, E. I. *J. Mol. Catal. A* **2002**, *177*, 179-194.

(19) Blümel, J. Lecture script "*Multinuclear High-Resolution and Solid-State NMR Spectroscopy*," Department of Texas A&M University, College Station, Texas, **2009**.

(20) Duncan, T. M. *A Compilation of Chemical Shift Anisotropies*; Farragut Press: Chicago, IL, **1990**.

(21) Emsley, L.; Laws, D. D.; Pines, A. *Angew. Chem. Int. Ed.* **2002**, *41*, 3096.

(22) Beele, B. *Ph.D. Dissertation*, University of Heidelberg, **2009**.

(23) Pines, A.; Gibby, M. G.; Waugh, I. S. *J. Chem. Phys*. **1973**, *59*, 569.

(24) Duer, J. M. *Solid-state NMR spectroscopy: principles and applications*; Blackwell Science, Oxford: Massachusetts, **2002**.

(25) Fitzgerald, J. J. *Solid-State NMR Spectroscopy of Inorganic Materials*; American Chemical Society: Washington DC, 1999.

(26) Lewanzik, N.; Oeser, T.; Blümel, J.; Gladysz, J. A. *J. Mol. Catal. A*. **2006**, *254*, 20-28.

(27) Song, C. E.; Lee. S. *Chem. Rev*. **2002**, *102*, 3495.

(28) McMorn, P.; Hutchings, G. J. *Chem. Soc. Rev*. **2004**, *33*, 108.

(29) Bianchini, C.; Barbaro, P.; Dal Santo, V.; Gobetto, R.; Meli, A.; Oberhauser, W.; Psaro, R.; Vizza, F. *Adv. Synth. Catal*. **2001**, *343*, 41.

(30) Horn, J.; Michalek, F.; Tzschucke, C. C.; Banwarth, W. *Topics in Current Chemistry* **2004**, *242*, 43.

(31) Arhancet, J. P.; Davis, M. E.; Merola, J. S.; Hanson, B. E. *Nature* **1898**, *339*, 454.

(32) (a) Bhange, B. M.; Shirai, M.; Arai, M. *J. Mol. Catal. A*. **1999**, *145*, 69. (b) Fujita, S.; Yoshida, T.; Bhange, B. M.; Shirai, M.; Arai, M. *J. Mol. Catal. A*. **2002**, *180*, 277.

(33) Quignard, F.; Larbot, S.; Goutodier, S.; Choplin, A. *J. Chem. Soc. Dalton Trans*. **2002**, 1147.

(34) Wan, K. T.; Davis, M. E. *Nature* **1994**, *370*, 449.

(35) (a) Klack, P.; Escaffre, P.; Serein-Spirau, F.; Thorez, A. *New J. Chem*. **1988**, *12*, 687. (b) Turov, V. V.; Leboda, R. *Adv. Colloid Interface Sci*. **1999**, *79*, 173.

(36) Mirza, A. R.; Anson, M. S.; Hellgardt, K.; Leese, M. P.; Thompson, D. F.; Tonks, Williams, J. M. J. *Org. Process Res. Dev*. **1998**, *2*, 325.

(37) Arends, I. W. C. E.; Sheldon, R. A. *Appl. Catal. A*. **2001**, *212*, 175.

(38) (a) Guillevic, M. A.; Rocaboy, C.; Arif, A. M.; Horvath, I. T.; Gladysz, J. A. *Organometallics* **1998**, *17*, 707. (b) Rutherford, D.; Juliette, J. J. J.; Rocaboy, C.; Horvath, I. T.; Gladysz, J. A. *Catalysis Today*. **1998**, *42*, 381. (c) Chechik, V.; Crooks, R. M. *J. Am. Chem. Soc*. **2000**, *122*, 1243.

(39) Tzschucke, C. C.; Markert, C.; Glatz, H.; Banwarth, W. *Angew. Chem. Int. Ed*. **2002**, *41*, 4500.

(40) (a) Bremeyer, N.; Ley, S. V.; Ramaro, C.; Shirley, I. M.; Smith, S. C. *Synlett* **2002**, 4500. (b) Yu, J. Q.; Wu, H. C.; Ramarao, C.; Spenncer, J. B.; Ley, S. V. *Chem. Commun.* **2003**, 678.

(41) Ley, S. V.; Ramaro, C.; Gordon, R. S.; Holmes, A. B.; Morrison, A. J.; McConvey, I. F.; Shirley, I. M.; Smith, S. C.; Smith, M. D. *Chem. Commun*. **2002**, 1134.

(42) Jamis, J.; Anderson, J. R.; Dickson, R. S.; Campi, E. M.; Jackson, W. R. *J. Organomet. Chem*. **2001**, *627*, 37.

(43) (a) Sabatier, M. J.; Corma, A.; Domenech, A.; Fornes, V.; Garcia, H. *Chem. Commun*. **1997**, 1285. (b) Ogunwami, S. B.; Bein, T. *Chem. Commun*. **1997**, 901.

(44) DeVos, D. E.; Thibault-Starzky, F.; Knops-Gerrits, P. P.; Parton, R. F.; Jacobs, P. A. *Macromol. Symp*. **1994**, *80*, 157.

(45) DeVos, D. E.; Vankelecom, I. F. J.; Jacobs, P. A. *Chiral Catalyst Immobilization and Recycling*, Wiley-VCH, Weinheim, Germany, **2000**.

(46) Benaglia, M.; Puglisi, A.; Cozzi, F. *Chem. Rev*. **2003**, *103*, 3401.

(47) McNamara, C. A.; Dixon, M .J.; Bradley, M. *Chem. Rev*. **2002**, *102*, 3275.

(48) (a) Gravert, D. J.; Janda, K. D. *Chem. Rev*. **1997**, *97*, 489. (b) Wentworth, J. P.; Janda, K. D. *Chem. Commun*. **1999**, 1917. (c) Haag, R. *Chem. Eur. J*. **2001**, *7*, 327.

(49) (a) Collman, J. P.; Hegedus, L. S.; Cooke, M. O.; Norton, J. R.; Dolcetti, G.; Marquardt, D. *J. Am. Chem. Soc*. **1972**, *94*, 1789. (b) Bayer, E.; Schurig, V. *Angew. Chem. Int. Ed*. **1975**, *14*, 493.

(50) Yao, Q. Angew. *Chem. Int. Ed*. **2000**, *39*, 3896.

(51) Bergbreiter, D.E. *Chem. Rev*. **2002**, *102*, 3345.

(52) Schlenk, C.; Kleij, A.W.; Frey, H.; Kotten, G. *Angew. Chem. Int. Ed*. **2000**, *39*, 3445.

(53) Schwab, E.; Mecking, S. *Organometallics* **2001**, *20*, 5504.

(54) Buhlier, W.; Wehner, W.; Voegtle, F. *Synthesis* **1978**, 155.

(55) Ulman, M.; Grubbs, R. H. *J. Org. Chem*. **1999**, *64*, 7202.

(56) Mukhopadhyah, S.; Rothenberg, G.; Gitis, D.; Sasson, Y. *J. Org. Chem*. **2000**, *65*, 3107.

(57) Fetouaki, R.; Seifert, A.; Bogza, M.; Oeser, T.; Blümel, J. *Inorg. Chim. Acta*. **2006**, *359*, 4865-4873.

(58) Bogza, M.; Oeser, T.; Blümel, J. *J. Organomet. Chem*. **2005**, *690*, 3383-3389.

(59) Posset, T.; Rominger, F.; Blümel, J. *Chem. Mater*. **2005**, *17*, 586-595.

(60) Brenna, S.; Posset, T.; Furrer, J.; Blümel, J. *Chem. Eur. J*. **2006**, *12*, 2880-2888.

(61) (a) Posset, T.; Blümel, J. *J. Am. Chem. Soc*. **2006**, *128*, 8394-8395. (b) Guenther, J.; Reibenspies, J.; Blümel, J. *Adv. Synth. Catal*. **2011**, *353*, 443-460.

(62) (a) Blümel, J. *J. Am. Chem. Soc*. **1995**, *117*, 2112-2113. (b) Behringer, K. D.; Blümel, J. *J. Liquid Chromatogr*. **1996**, *19*, 2753-2765.

(63) Fournier, J. H.; Maris, T.; Wuest, J. D.; Guo, W. Z.; Galoppini, E. *J. Am. Chem. Soc.* **2003**, *125*, 1002.

(64) Vasylyev, M.; Wachtel, E. J.; Popovitz-Biro, R.; Neumann, R. *Chem. Eur. J*. **2006**, *12*, 3507.

(65) Wang, S.; Oldham, W. J.; Hudack, R. A.; Bazan, G. C. *J. Am. Chem. Soc.* **2000**, *122*, 5695.

(66) Yeh, H. C.; Lee, R. H.; Chan, L. H.; Lin, T. Y. J.; Chen, C. T.; Balasubramaniam, E.; Tao, Y.-T. *Chem. Mater.* **2001**, *13*, 2788.

(67) Eng, G.; Zhang, Y. Z.; Whalen, D.; Ramsammy, R.; Khoo, L. E.; DeRosa, M. *Appl. Organomet. Chem.* **1994**, *8*, 445.

(68) Wander, M.; Hausoul, P. J. C.; Sliedregt, L. A. J. M.; van Stehen, B. J.; van Koten, G.; Klein Gebbink, R. J. M. *Organometallics* **2009**, *28*, 4406.

(69) Zhang, B.; Wang, Z.; Wang, Z.; Li, J.; Leng, S.; Shen, C.; Jiang, Y. *Polymer* **2009**, *50*, 2025.

(70) Yang, Y. *Ph.D. Dissertation*, University of Heidelberg, **2007**.

(71) Wiench, J. W.; Michon, C.; Ellern, A.; Hazendonk, P.; Iuga, A.; Angelici, R. J.; Pruski, M. *J. Am. Chem. Soc*. **2009**, *131*, 11801-11810.

(72) Eichele, K.; Wasylishen, R. E. *WSolids1*; Dalhouise University: Halifax, Canada.

(73) Sommer, J.; Yang, Y.; Rambow, D.; Blümel, J. *Inorg. Chem.* **2004**, *43*, 7561-7563.

(74) Wrackmeyer, B. *Ann. R. NMR S.* **1999**, *38*, 203-269.

(75) Stach, M. *Diploma thesis*, University of Heidelberg, **2009**.

APPENDIX

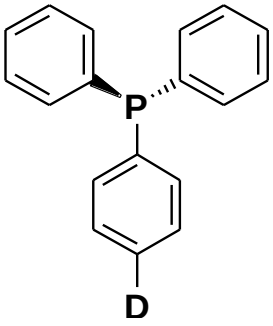

3-2

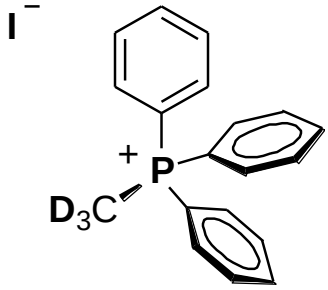

3-3

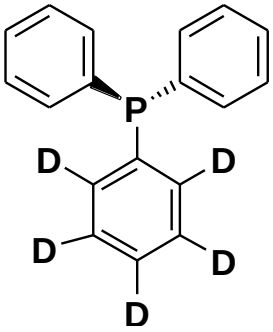

3-10

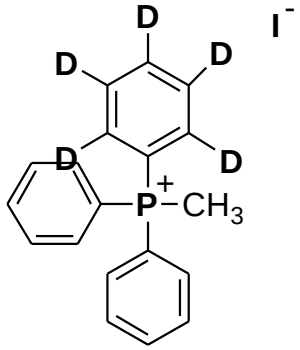

3-11

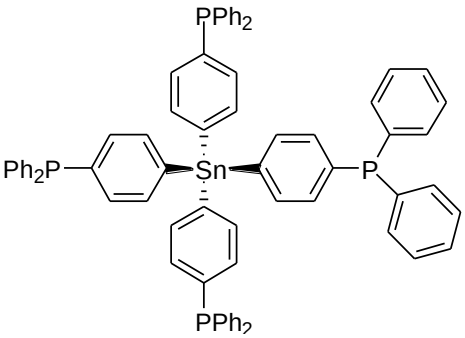

3-12

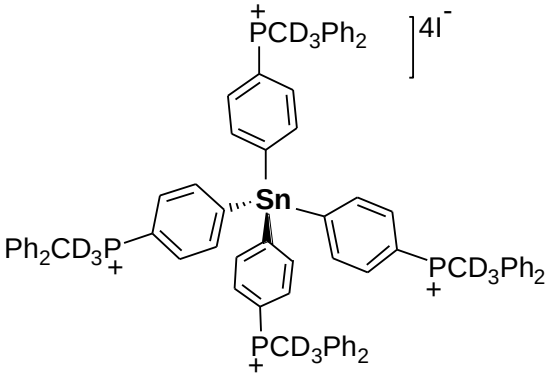

3-13

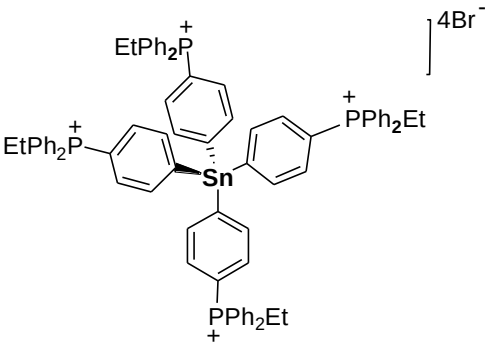

3-14

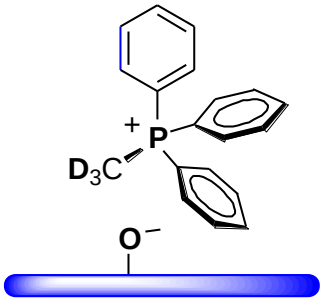

3-3i

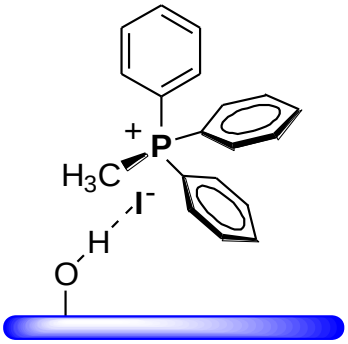

3-4i

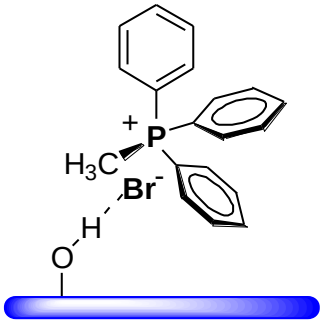

3-5i

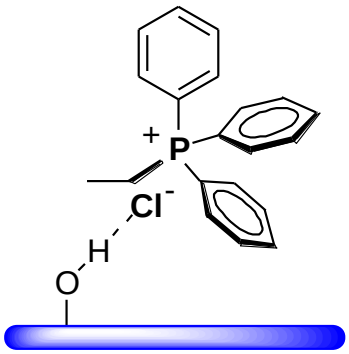

3-6i

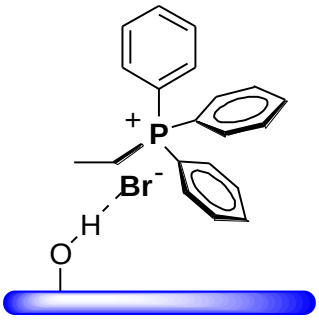

3-7i

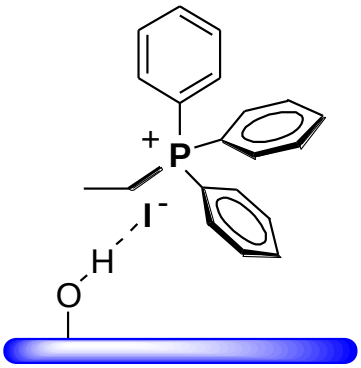

3-8i

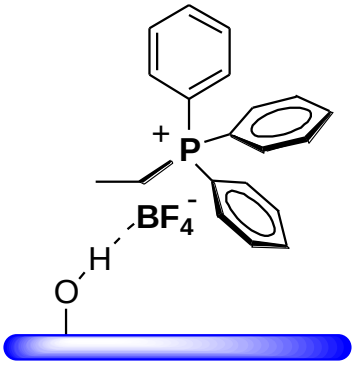

3-9i

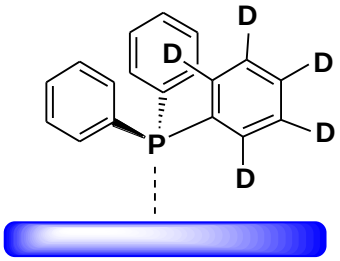

3-10a

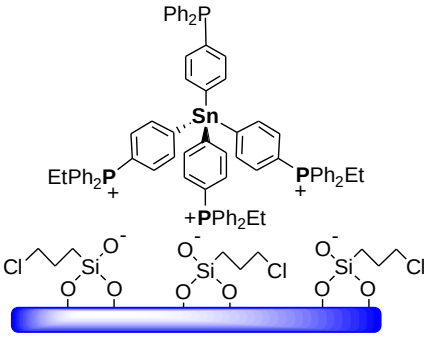

3-12i

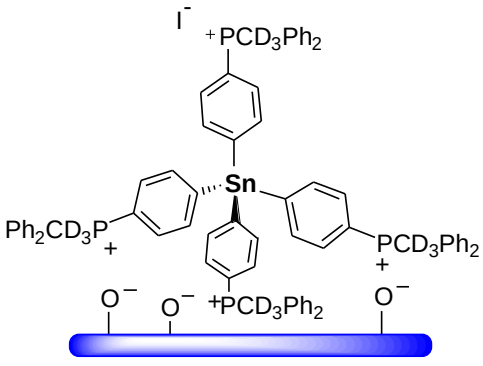

3-13i

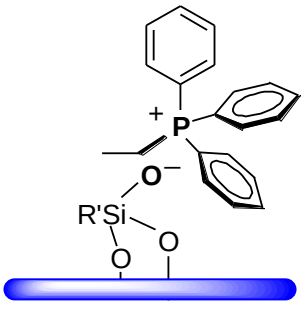

3-15i

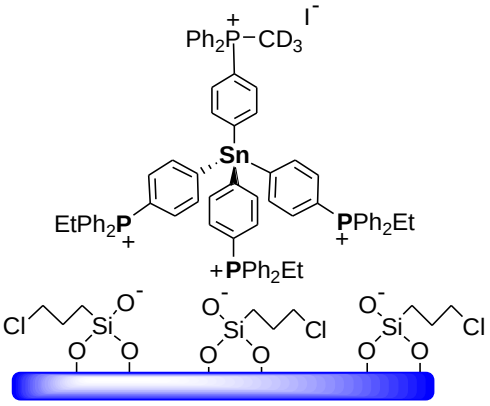
Ph2P−CD3
I
Sn
EtPh2P
PPh2Et
PPh2Et
Cl
Si
O
Cl
Cl

3-16i

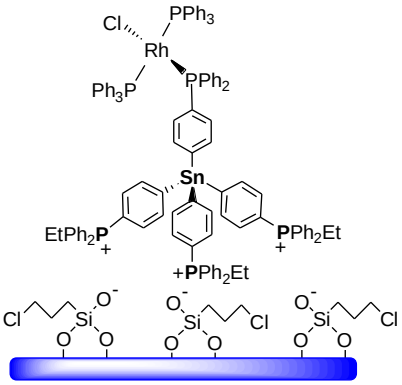
Cl
Rh
PPh3
Ph3P
PPh2
Sn
EtPh2P
PPh2Et
PPh2Et
Cl
Si
O
Cl
Cl

3-17i

VITA

Melanie Ingrid Perera received her Bachelor of Science degree in Chemistry from Wheeling Jesuit University in 2007. She entered the chemistry program at Texas A&M University in August 2007 and received her Master of Science degree in August 2011. Her research interests include inorganic chemistry, heterogeneous catalysts on a SiO_2 support, solid-state NMR, and mobility studies using ^2H solid-state NMR. Ms. Perera may be reached at Texas A&M University, Department of Chemistry, P. O. Box 30012, College Station, Texas 77842-3012. Her email is mymel320@gmail.com.